AD_____

Award Number: W81XWH-09-2-0105

TITLE: Nrdp1-Mediated ErbB3 Increase During Androgen Ablation and Its Contribution to Androgen-Independence

PRINCIPAL INVESTIGATOR: Paramita M. Ghosh, Ph.D.

CONTRACTING ORGANIZATION: University of California
Davis, CA 95616

REPORT DATE: September 2012

TYPE OF REPORT: Annual

PREPARED FOR: U.S. Army Medical Research and Materiel Command
Fort Detrick, Maryland 21702-5012

REPORT DOCUMENTATION PAGE

Form Approved
OMB No. 0704-0188

1. REPORT DATE	2. REPORT TYPE	3. DATES COVERED
September 2012	Annual	15 August 2011 – 14 August 2012

4. TITLE AND SUBTITLE

Nrdp1-Mediated ErbB3 Increase During Androgen Ablation and Its Contribution to Androgen-Independence

5a. CONTRACT NUMBER

5b. GRANT NUMBER
W81XWH-09-2-0105

5c. PROGRAM ELEMENT NUMBER

6. AUTHOR(S)

Paramita M. Ghosh, Ph.D.

E-Mail: paghosh@ucdavis.edu

5d. PROJECT NUMBER

5e. TASK NUMBER

5f. WORK UNIT NUMBER

7. PERFORMING ORGANIZATION NAME(S) AND ADDRESS(ES)

University of California, Davis
Davis, CA 95616

8. PERFORMING ORGANIZATION REPORT NUMBER

9. SPONSORING / MONITORING AGENCY NAME(S) AND ADDRESS(ES)
U.S. Army Medical Research and Materiel Command
Fort Detrick, Maryland 21702-5012

10. SPONSOR/MONITOR'S ACRONYM(S)

11. SPONSOR/MONITOR'S REPORT NUMBER(S)

12. DISTRIBUTION / AVAILABILITY STATEMENT
Approved for Public Release; Distribution Unlimited

13. SUPPLEMENTARY NOTES

14. ABSTRACT
Despite availability of improved androgen receptor (AR) inhibitors for the treatment of castration-resistant prostate cancer (CRPC), resistance to treatment develops, and has been traced to activation of multiple signaling pathways suppressed by the AR. We previously showed that the AR maintained castration sensitivity in prostate cancer (PCa) by transcriptional regulation of the E3 ubiquitin ligase Nrdp1, which degrades the receptor tyrosine kinase (RTK) ErbB3; whereas AR inhibition suppressed Nrdp1 levels, thereby activating ErbB3. This resulted in CRPC growth and AR stimulation, but in CRPC, the AR was unable to regulate Nrdp1 or suppress ErbB3, causing uncontrolled progression. Here, we investigate the mechanism by which the AR regulates Nrdp1 transcription and why this regulation is lost in CRPC. Immunohistochemical studies in human PCa tissue and in PCa mouse models demonstrated Nrdp1 localization in both nucleus and cytoplasm. In vitro studies determined cytoplasmic Nrdp1 is 36kDa while nuclear Nrdp1 is 28kDa; the 36kDa form, but not the 28kDa form, negatively correlated with ErbB3 levels, but both forms positively correlated with AR. We demonstrate that Nrdp1 is a direct transcriptional target of the AR in androgen-dependent cells expressing a truncated form of the structural protein Filamin A (FlnA) in the nucleus, but in CRPC cells which have lost nuclear FlnA expression, the AR is no longer able to bind to the Nrdp1 promoter. Restoration of nuclear FlnA restored the ability of AR to regulate Nrdp1 transcription. Thus dual targeting of ErbB3 and AR may be effective in patients whose tumors express nuclear FlnA.

15. SUBJECT TERMS
ErbB3, Akt, cell proliferation, cell survival, androgen withdrawal, androgen receptor, EGFR, ErbB2, LNCaP, Nrdp1, RNF41, HER2, HER3, androgen response element, FKHRL1. transcriptional activity

16. SECURITY CLASSIFICATION OF:			17. LIMITATION OF ABSTRACT	18. NUMBER OF PAGES	19a. NAME OF RESPONSIBLE PERSON
a. REPORT	b. ABSTRACT	c. THIS PAGE			USAMRMC
U	U	U	UU	56	19b. TELEPHONE NUMBER *(include area code)*

Table of Contents

INTRODUCTION: Patients with advanced prostate cancer (PCa) are initially susceptible to androgen withdrawal therapy (AWT), but ultimately develop resistance to this therapy (castration-resistant PCa, CRPC). The treatment options for patients who fail AWT are limited; hence the long-term goal of these studies is to identify therapeutic strategies to prolong the effectiveness of AWT. The ErbB receptor tyrosine kinase (RTK) family regulates proliferation and survival in PCa. Multiple studies suggested that ErbB3 plays a role in promoting PCa, however, its mechanism of action and the pathways mediating its effects were unknown. Hence, we investigate the role of ErbB3 in PCa progression.

BODY:

Specific Aim 1. To test the hypothesis that increased ErbB3 during androgen ablation results in androgen independence of prostate cancer cells.

Task 1: *We will examine in paraffin embedded prostate cancer tissues (human anatomical samples) whether there is increased ErbB3 and decreased Nrdp1 expression in androgen independent tumors from human patients.* ***(Months 1-9)***

Complete – report in previous Annual Report (2010).

Task 2: *In an animal model of prostate cancer progression, we will investigate whether inhibition of ErbB3 during androgen ablation prevents the development of CRPC tumors.* ***(Months 9-18)***

Partial report in previous Annual Report (2010). In that report, we showed that androgen ablation caused an increase in ErbB3 levels in the CWR22 mouse xenograft model of prostate cancer.

Complete – report in previous Annual Report (2011).

Specific Aim 2. To test the hypothesis that Nrdp1 mediates the regulation of ErbB3 expression by the androgen receptor in androgen dependent cells, but this regulation is lost in androgen independence.

Task 3: *We will identify a role for Nrdp1 in the expression of ErbB3 during androgen withdrawal and in androgen independence.* ***(Months 1-12)***

Complete – report in previous Annual Report (2010)

Task 4: *In androgen dependent cells we will determine how the androgen receptor regulates Nrdp1 transcription.* ***(Months 13-24)***

Outcomes: A manuscript on this topic is prepared and is in the last phase of submission, the manuscript is attached.

Task 5: *In addition, in androgen independent cells we will identify the cause for repression of Nrdp1 expression and investigate whether ErbB3, Akt or its downstream effector FKHRL1 plays a role in this process.* ***(Months 25-36)***

Status: Ongoing. These studies will be completed soon and will be presented in the final report in February, 2013.

REPORTABLE OUTCOMES:

1. Manuscript prepared for publication.
2. Qualifying Exam: Maitreyee Jathal who was supported by this project is going to take her qualifying exams in January 2013.

CONCLUSION: Our data for the first time identifies Nrdp1 as an AR target that is androgen-regulated in castration resistant cells, but not in castration insensitive cells. Our new data shows that in cells where the AR is stabilized, and does not undergo degradation despite androgen withdrawal, it is able to transcribe PSA but not Nrdp1, whereas in cells where the AR is not stabilized, it can transcribe Nrdp1 and thereby regulate ErbB3 levels. Since we also showed earlier that ErbB3 signaling increase cell growth and suppress apoptosis, our results indicate that AR suppression of ErbB3 is a mechanism for keeping cells castration sensitive, whereas when this effect is lost, the cells become castration resistant. Further, we show that Filamin A nuclear localization keeps cells androgen responsive by destabilizing the AR, and maintaining its ability to transcriptionally regulate Nrdp1.

APPENDICES:

Manuscript about to be submitted.

SUPPORTING DATA: See above (included in text).

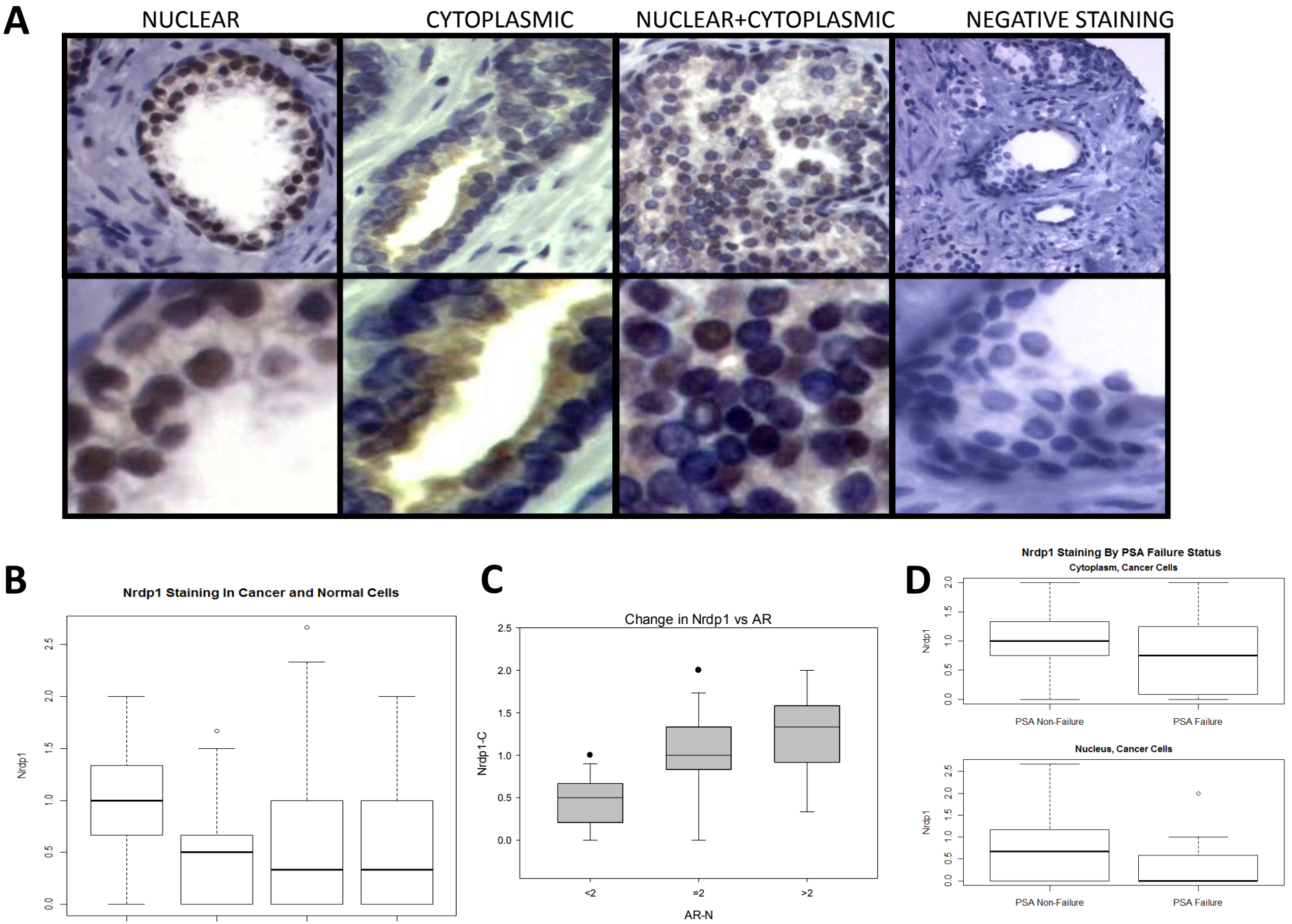
A
NUCLEAR
CYTOPLASMIC
NUCLEAR+CYTOPLASMIC
NEGATIVE STAINING
B
Nrdp1 Staining In Cancer and Normal Cells
Nrdp1
0.0
0.5
1.0
1.5
2.0
2.5
Cytoplasm, CA
Cytoplasm, No CA
Nucleus, CA
Nucleus, No CA
C
Change in Nrdp1 vs AR
Nrdp1-C
0.0
0.5
1.0
1.5
2.0
2.5
<2
=2
>2
AR-N
D
Nrdp1 Staining By PSA Failure Status
Cytoplasm, Cancer Cells
Nrdp1
0.0
0.5
1.0
1.5
2.0
PSA Non-Failure
PSA Failure
Nucleus, Cancer Cells
Nrdp1
0.0
0.5
1.0
1.5
2.0
2.5
PSA Non-Failure
PSA Failure

FIGURE 1

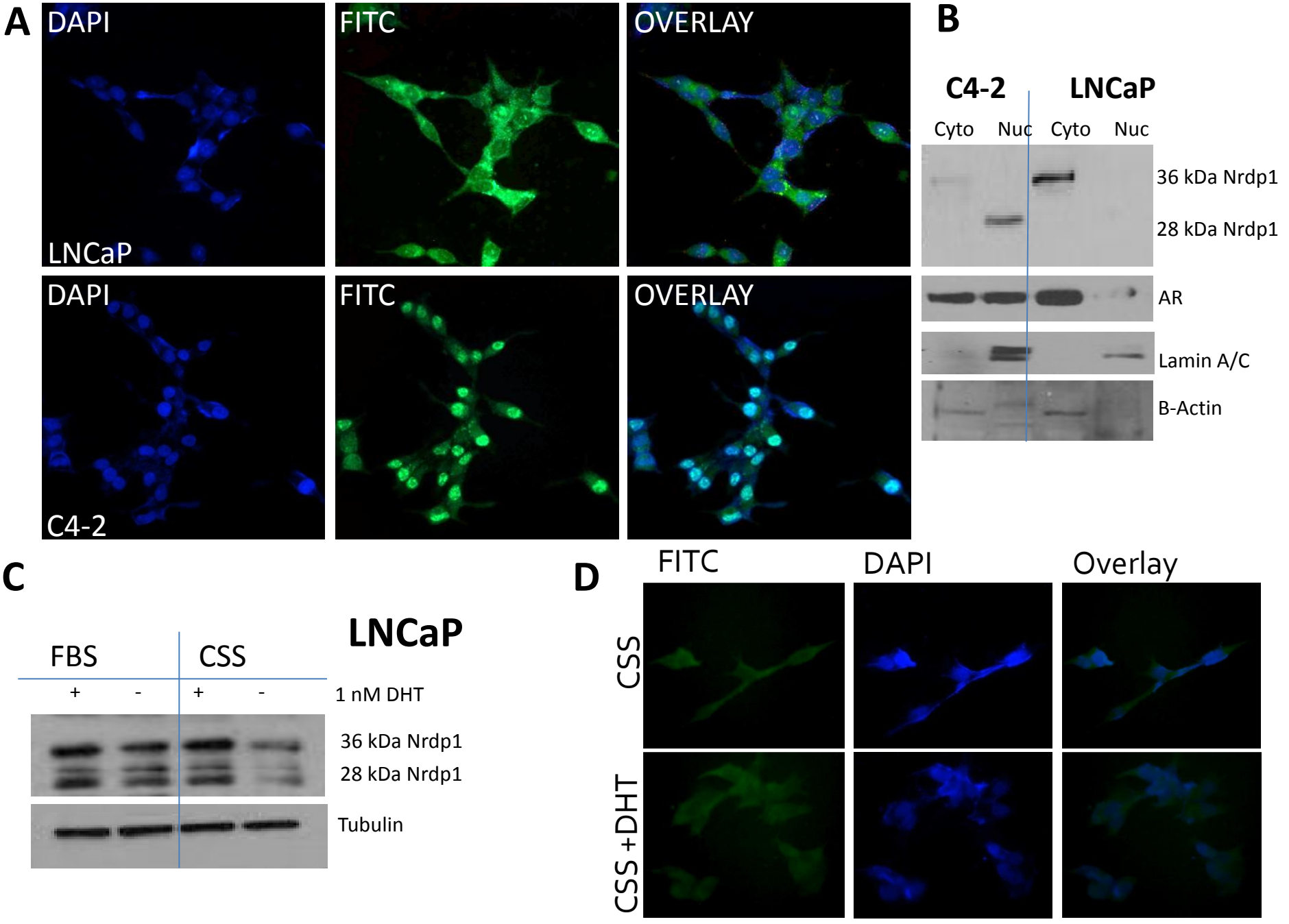
A
DAPI
FITC
OVERLAY
LNCaP
DAPI
FITC
OVERLAY
C4-2
B
C4-2
LNCaP
Cyto
Nuc
Cyto
Nuc
36 kDa Nrdp1
28 kDa Nrdp1
AR
Lamin A/C
B-Actin
C
LNCaP
FBS
CSS
+
-
+
-
1 nM DHT
36 kDa Nrdp1
28 kDa Nrdp1
Tubulin
D
FITC
DAPI
Overlay
CSS
CSS +DHT

FIGURE 2

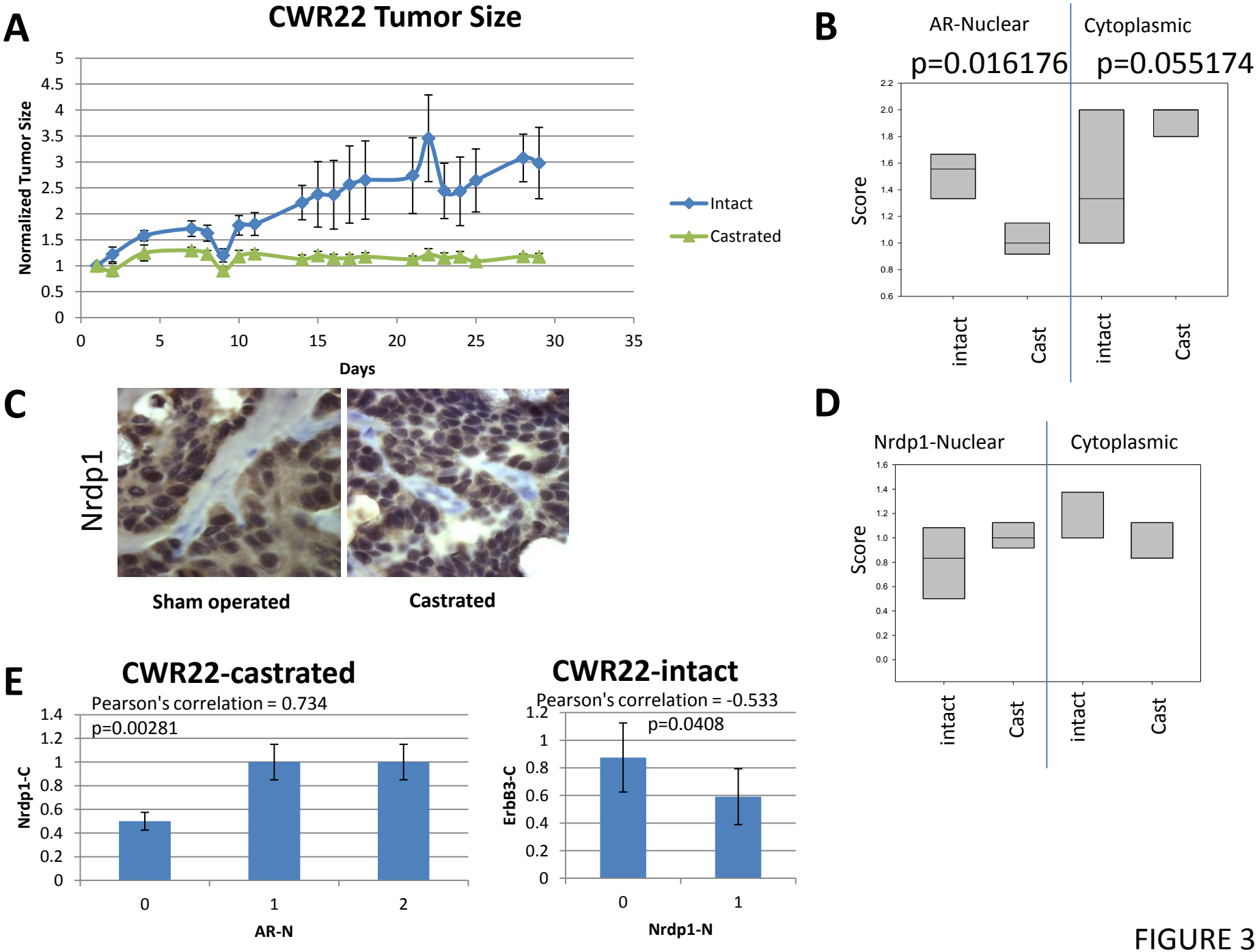
A
CWR22 Tumor Size
Normalized Tumor Size
Days
Intact
Castrated
B
AR-Nuclear
Cytoplasmic
p=0.016176
p=0.055174
Score
intact
Cast
intact
Cast
C
Nrdp1
Sham operated
Castrated
D
Nrdp1-Nuclear
Cytoplasmic
Score
intact
Cast
intact
Cast
E
CWR22-castrated
Pearson's correlation = 0.734
p=0.00281
Nrdp1-C
AR-N
CWR22-intact
Pearson's correlation = -0.533
p=0.0408
ErbB3-C
Nrdp1-N

FIGURE 3

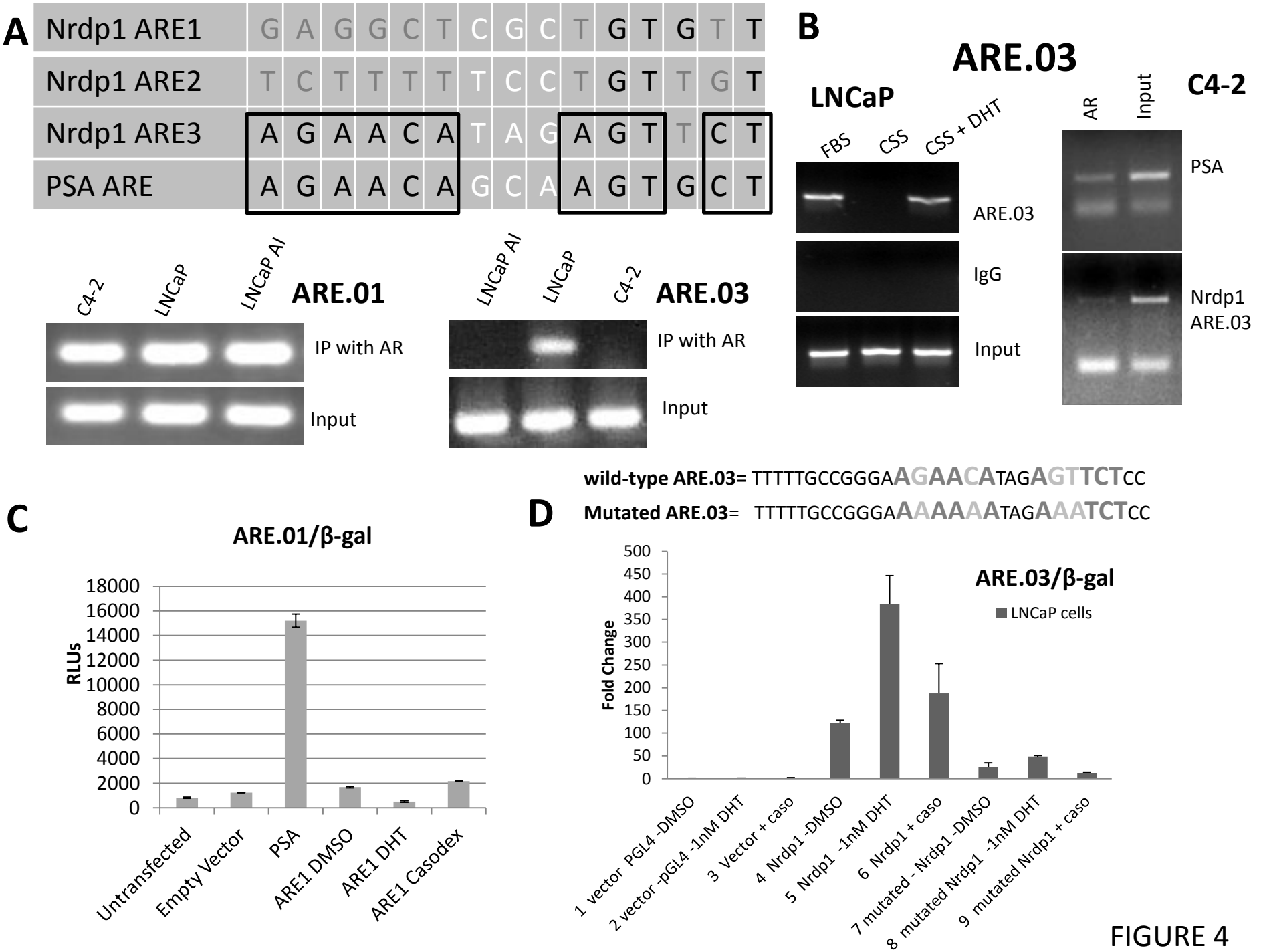
A
Nrdp1 ARE1 G A G G C T C G C T G T G T T
Nrdp1 ARE2 T C T T T T T C C T G T T G T
Nrdp1 ARE3 A G A A C A T A G A G T T C T
PSA ARE A G A A C A G C A A G T G C T
B
ARE.03
LNCaP
FBS
CSS
CSS + DHT
ARE.03
IgG
Input
C4-2
AR
Input
PSA
Nrdp1 ARE.03
C4-2
LNCaP
LNCaP AI
ARE.01
IP with AR
Input
LNCaP AI
LNCaP
C4-2
ARE.03
IP with AR
Input
wild-type ARE.03= TTTTTGCCGGGAAGAACATAGAGTTCTCC
Mutated ARE.03= TTTTTGCCGGGAAAAAAATAGAAATCTCC
C
ARE.01/β-gal
RLUs
18000
16000
14000
12000
10000
8000
6000
4000
2000
0
Untransfected
Empty Vector
PSA
ARE1 DMSO
ARE1 DHT
ARE1 Casodex
D
ARE.03/β-gal
LNCaP cells
Fold Change
500
450
400
350
300
250
200
150
100
50
0
1 vector PGL4 -DMSO
2 vector -pGL4 -1nM DHT
3 Vector + caso
4 Nrdp1 -DMSO
5 Nrdp1 -1nM DHT
6 Nrdp1 + caso
7 mutated - Nrdp1 -DMSO
8 mutated Nrdp1 -1nM DHT
9 mutated Nrdp1 + caso

FIGURE 4

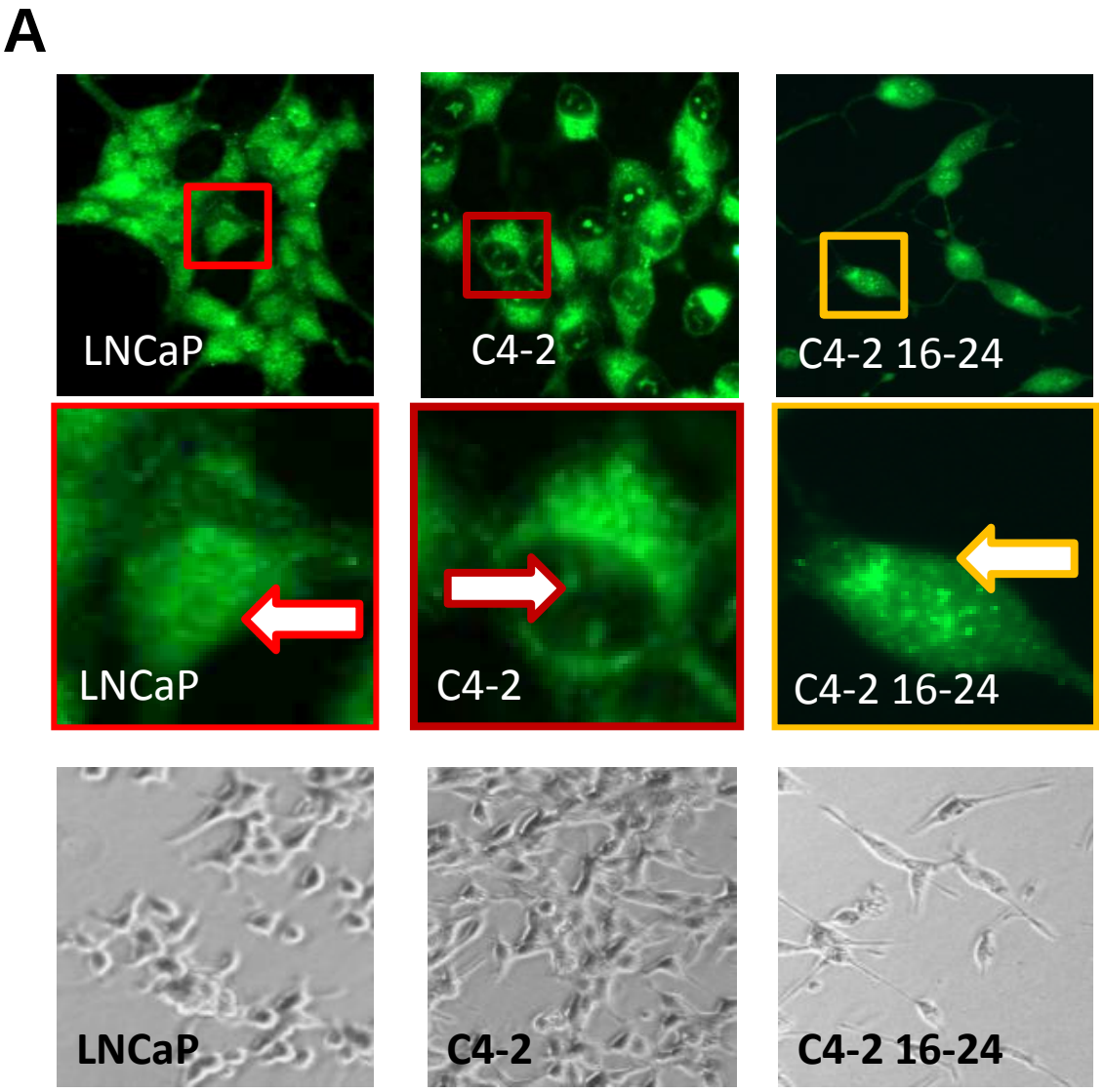
A
LNCaP
C4-2
C4-2 16-24
LNCaP
C4-2
C4-2 16-24
LNCaP
C4-2
C4-2 16-24

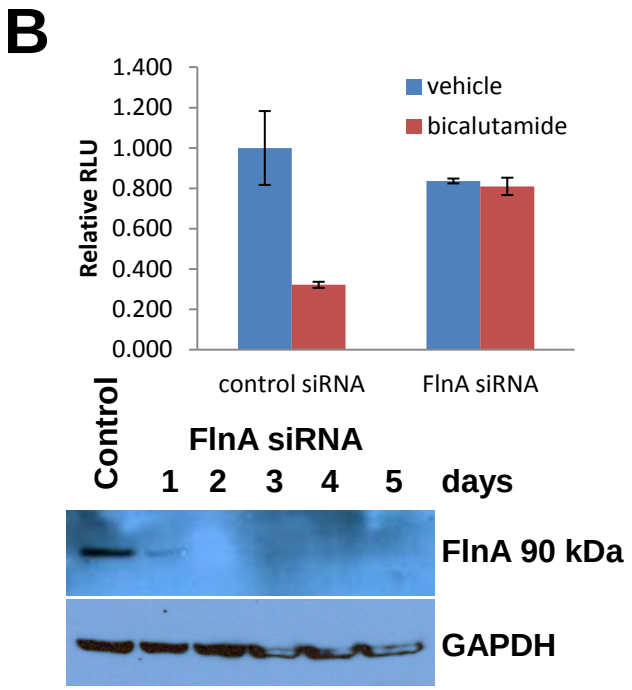
B
Relative RLU
1.400
1.200
1.000
0.800
0.600
0.400
0.200
0.000
vehicle
bicalutamide
control siRNA
FlnA siRNA
Control
FlnA siRNA
1 2 3 4 5 days
FlnA 90 kDa
GAPDH

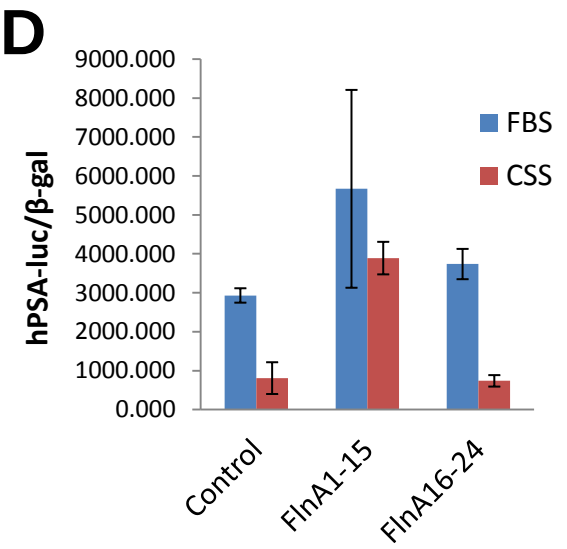
D
hPSA-luc/β-gal
9000.000
8000.000
7000.000
6000.000
5000.000
4000.000
3000.000
2000.000
1000.000
0.000
FBS
CSS
Control
FlnA1-15
FlnA16-24

FIGURE 5

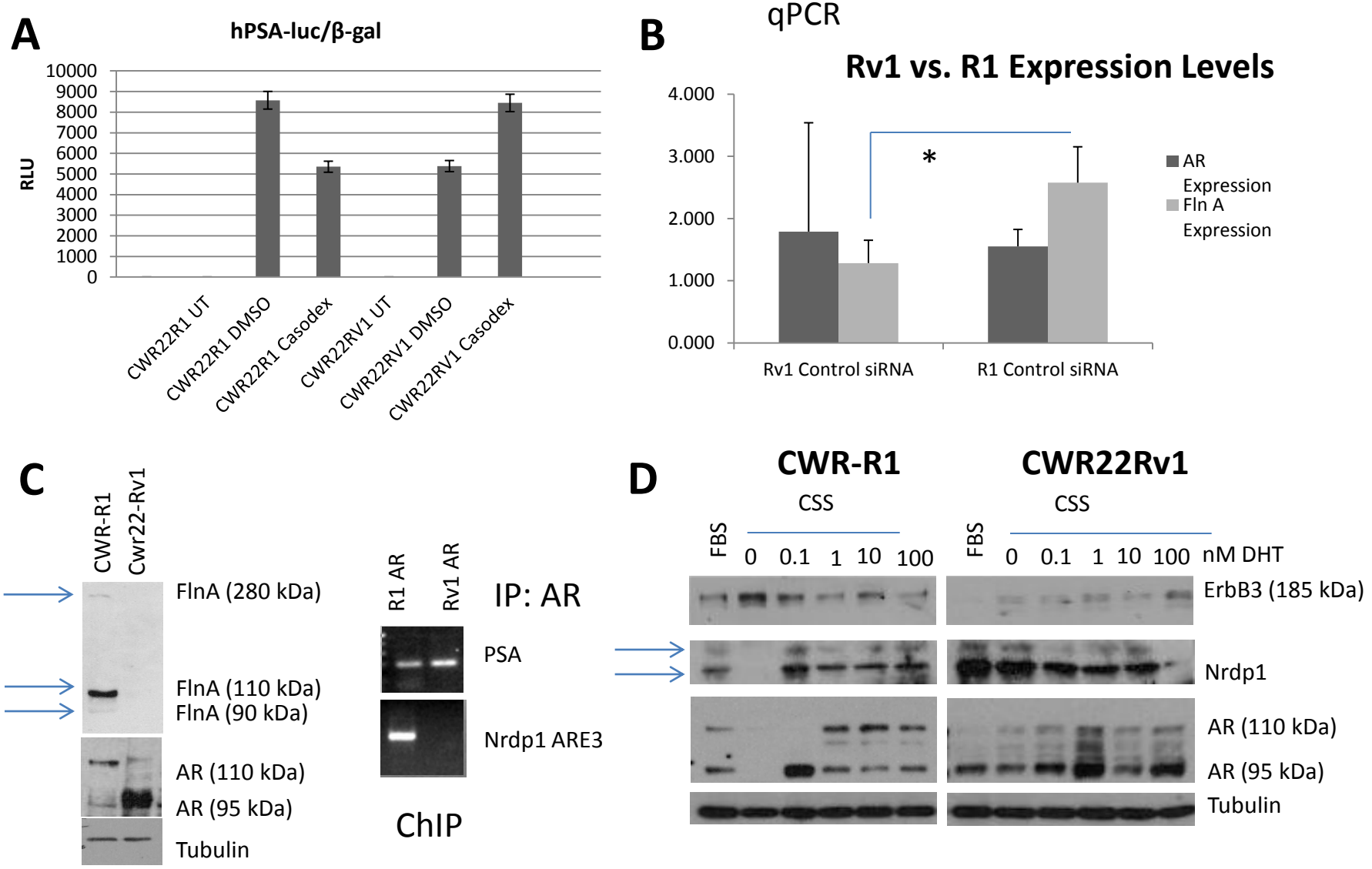
A
hPSA-luc/β-gal
RLU
10000
9000
8000
7000
6000
5000
4000
3000
2000
1000
0
CWR22R1 UT
CWR22R1 DMSO
CWR22R1 Casodex
CWR22RV1 UT
CWR22RV1 DMSO
CWR22RV1 Casodex
B
qPCR
Rv1 vs. R1 Expression Levels
4.000
3.000
2.000
1.000
0.000
*
AR Expression
Fln A Expression
Rv1 Control siRNA
R1 Control siRNA
C
CWR-R1
Cwr22-Rv1
FlnA (280 kDa)
FlnA (110 kDa)
FlnA (90 kDa)
AR (110 kDa)
AR (95 kDa)
Tubulin
R1 AR
Rv1 AR
IP: AR
PSA
Nrdp1 ARE3
ChIP
D
CWR-R1
CWR22Rv1
CSS
FBS
0
0.1
1
10
100
nM DHT
ErbB3 (185 kDa)
Nrdp1
AR (110 kDa)
AR (95 kDa)
Tubulin

FIGURE 6

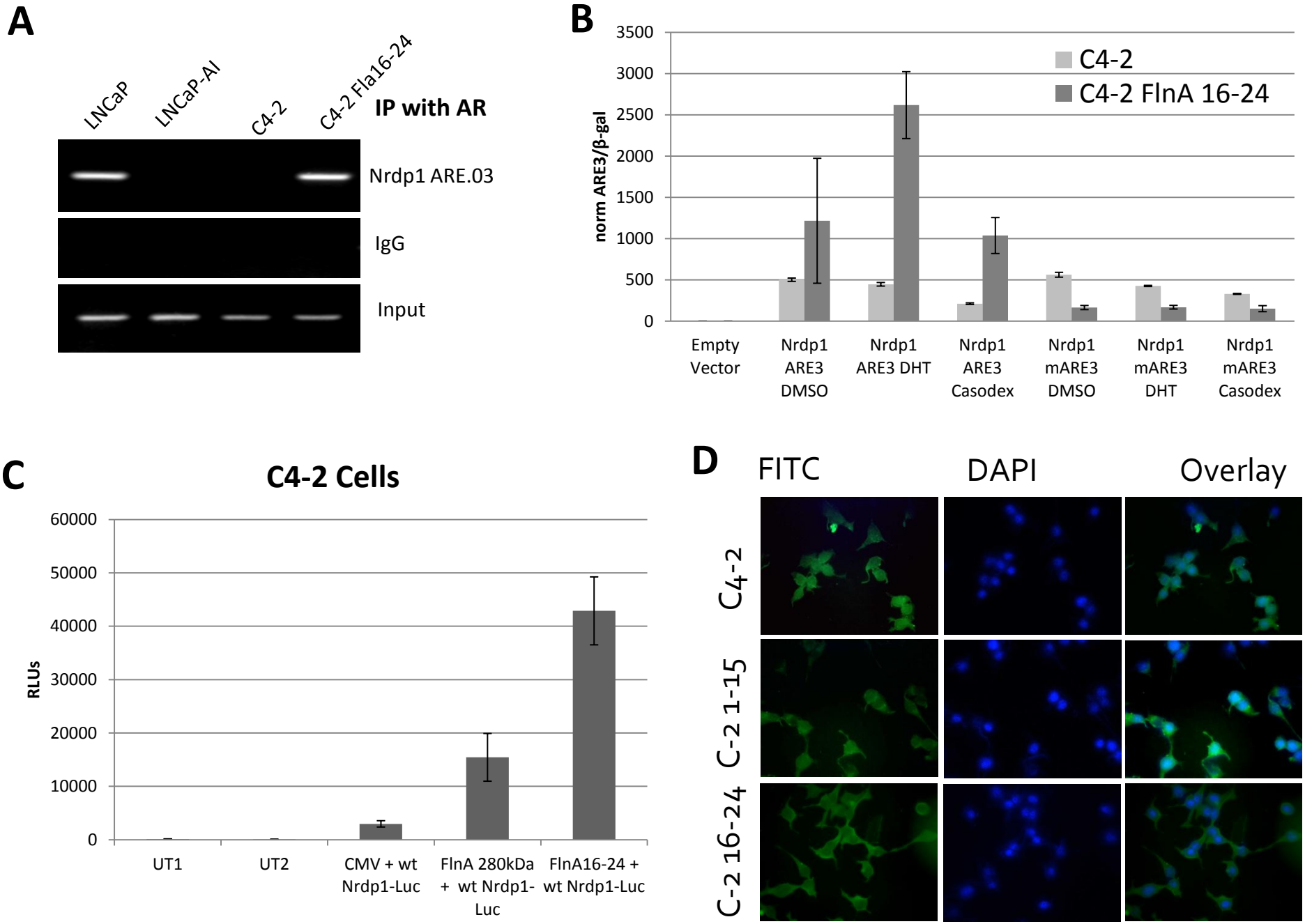
A
LNCaP
LNCaP-AI
C4-2
C4-2 Fla16-24
IP with AR
Nrdp1 ARE.03
IgG
Input
B
norm ARE3/β-gal
3500
3000
2500
2000
1500
1000
500
0
C4-2
C4-2 FlnA 16-24
Empty Vector
Nrdp1 ARE3 DMSO
Nrdp1 ARE3 DHT
Nrdp1 ARE3 Casodex
Nrdp1 mARE3 DMSO
Nrdp1 mARE3 DHT
Nrdp1 mARE3 Casodex
C
C4-2 Cells
RLUs
60000
50000
40000
30000
20000
10000
0
UT1
UT2
CMV + wt Nrdp1-Luc
FlnA 280kDa + wt Nrdp1-Luc
FlnA16-24 + wt Nrdp1-Luc
D
FITC
DAPI
Overlay
C4-2
C-2 1-15
C-2 16-24

FIGURE 7

Androgen receptor transcriptionally targets the ErbB3 regulator Nrdp1 in the presence of nuclear Filamin A

Rosalinda M. Savoy[1], Liqun Chen[1,4], Salma Siddiqui[4], Frank U. Melgoza[4], Blythe Durbin-Johnson[3], Mohana Roy[4], Maitreyee K. Jathal[1], Swagata Bose[1], Yu Wang[1], Benjamin A. Mooso[1,4], Leandro D'Abronzo[1], William H. Fry[2], Kermit L. Carraway, III[2], and *Paramita M. Ghosh[1,2,4].*

[1]Dept. of Urology, [2]Dept. of Biochemistry and Molecular Medicine, and [3]Division of Biostatistics, Department of Public Health Sciences University of California, Davis, CA, and [4]VA Northern California Health Care System, Mather, CA

Running Title: AR regulates Nrdp1 with nuclear Filamin A

Keywords: EGFR/HER2/HER3/AR/FLRF/RNF41/ABP280

Corresponding Author:

Paramita M. Ghosh, Ph.D.
Department of Urology
University of California Davis School of Medicine
4860 Y Street, Suite 3500
Sacramento, CA 95817
Phone: (916)843-9336
Fax: (916)364-0306
e-mail: paramita.ghosh@ucdmc.ucdavis.edu

ABSTRACT

Despite availability of improved androgen receptor (AR) inhibitors for the treatment of castration-resistant prostate cancer (CRPC), resistance to treatment develops, and has been traced to activation of multiple signaling pathways suppressed by the AR. We previously showed that the AR maintained castration sensitivity in prostate cancer (PCa) by transcriptional regulation of the E3 ubiquitin ligase Nrdp1, which degrades the receptor tyrosine kinase (RTK) ErbB3; whereas AR inhibition suppressed Nrdp1 levels, thereby activating ErbB3. This resulted in CRPC growth and AR stimulation, but in CRPC, the AR was unable to regulate Nrdp1 or suppress ErbB3, causing uncontrolled progression. Here, we investigate the mechanism by which the AR regulates Nrdp1 transcription and why this regulation is lost in CRPC. Immunohistochemical studies in human PCa tissue and in PCa mouse models demonstrated Nrdp1 localization in both nucleus and cytoplasm. I*n vitro* studies determined cytoplasmic Nrdp1 is 36kDa while nuclear Nrdp1 is 28kDa; the 36kDa form, but not the 28kDa form, negatively correlated with ErbB3 levels, but both forms positively correlated with AR. We demonstrate that *Nrdp1* is a direct transcriptional target of the AR in androgen-dependent cells expressing a truncated form of the structural protein Filamin A (FlnA) in the nucleus, but in CRPC cells which have lost nuclear FlnA expression, the AR is no longer able to bind to the *Nrdp1* promoter. Restoration of nuclear FlnA restored the ability of AR to regulate Nrdp1 transcription. Thus dual targeting of ErbB3 and AR may be effective in patients whose tumors express nuclear FlnA.

INTRODUCTION:

AR inhibition is a cornerstone of treatment for recurrent or advanced PCa; and initially the patient is treated with androgen withdrawal therapy (AWT), which hinges on the reduction of circulating androgen levels [1]. Although effective at first, patients undergoing AWT ultimately fail this therapy due to the development of CRPC, which is typically characterized by increased AR transcriptional activity giving rise to elevated levels of prostate specific antigen (PSA) in the serum [2, 3]. Patients with CRPC undergo additional treatment including chemotherapy [4], immunotherapy [5], and stronger AR inhibitors Abiraterone acetate [6, 7] and enzalutamide [8]. However, resistance to even the strongest available AR inhibitors set in quickly and multiple studies have been undertaken to investigate the cause of this resistance [9]. It was found that multiple cell signaling pathways that lead to increased cell proliferation and survival, as well as increased ligand-independent AR transcriptional activity, are activated when AR is inhibited [10-12]. Activation of each of these pathways result in tumor progression despite continued treatment, hence we investigated the source of this increased activity.

We previously showed that AR inhibition leads to upregulation of ErbB3 [12] which, similar to EGFR, is activated by ligand binding, and requires dimerization with other members of the family (EGFR, ErbB2, ErbB4) for complete action [13]. The expression of ErbB3 increased in tumor tissue compared to normal and is further increased in CRPC [12]. Increased ErbB3 resulted in improved growth and survival and also augmented AR transcriptional activity on a PSA promoter. Therefore, regulation of ErbB3 is of utmost importance in PCa. We also showed that in androgen-dependent cells, the AR suppresses ErbB3 levels by stimulating the transcription of an E3 ubiquitin ligase, Nrdp1 (also called RNF41 or FLRF) [12], which is known to regulate the degradation of ErbB3 [14, 15]. Recently, Carver et al [10] showed the presence of a reciprocal feedback loop in which PI3K pathway inhibition activates AR signaling by relieving feedback inhibition of HER kinases, especially ErbB3.

We reason that the AR normally suppresses ErbB3 in androgen-dependent cells as a mechanism of preventing bypass pathways that result in CRPC. However, in CRPC, this mechanism is

altered and the AR is no longer able to regulate Nrdp1 [12]. This causes unregulated ErbB3 expression and activation of pathways downstream of this RTK. In this project, we address why the AR regulates Nrdp1 in androgen-dependent but not in castration-resistant PCa. We show that the regulation of Nrdp1 by the AR requires the presence of a structural protein, Filamin A (FlnA) in the nucleus. We previously showed that FlnA is present in the nuclei of androgen-dependent but not castration-resistant PCa [16]. Nuclear FlnA promoted androgen-dependent cell growth, whereas the cells became castration-resistant in its absence [17]. However, restoration of FlnA in the nucleus restored androgen-dependent cell growth [17]. Full-length FlnA (280kDa) is cytoplasmic, whereas cleavage of this protein to a 90kDa fragment allows nuclear localization of the cleaved product [18]. Recently, we showed that FlnA cleavage is AR regulated and AR inhibition prevents its cleavage and nuclear localization [19]. Here, we demonstrate that restoration of FlnA nuclear localization restored the ability of the AR to regulate *Nrdp1* transcription, thereby showing that FlnA directly regulates the AR transcription program.

Previous studies had indicated that the AR regulates a distinct transcription program in CRPC compared to androgen-dependent cells [20]. For example, the AR selectively upregulates M-phase cell-cycle genes in CRPC cells that it does not in androgen-dependent cells. Our current data supports this observation and indicates that recruitment of suitable co-regulators, either activators or suppressors, likely determine the program that the AR regulates.

MATERIALS AND METHODS

***Cell culture and materials*:** LNCaP, CWR22Rv1 (ATCC, Manassas, VA), C4-2 (Urocor, Oklahoma City, OK), CWR22R1, LNCaP AI, RWPE1, PC3, DU145 cells were cultured in RPMI 1640 medium with 5% fetal bovine serum and 1% antibiotic-antimycotic solutions. HEK 293T cells were from Thermo Scientific. Cells were transiently transfected using Lipofectamine 2000 reagent (Invitrogen, Grand Island, NY) according to manufacturer's specifications based on established protocols using 1µg plasmid DNA The following plasmids were used in the transfections: pCMV-FlnA, FlnA(16-24) and FlnA(1-15) plasmids were kindly provided by Dr. E.W. Yong, National University of Singapore, Singapore. Human PSA-luciferase construct (hPSA-luc) was kindly provided by Dr. XuBao Shi, University of California Davis, Dept of Urology. An shRNA to Nrdp1 has been described earlier [15]. Casodex (bicalutamide) was kindly provided by AstraZeneca, Cheshire, UK. Dihydrotestosterone (DHT) was obtained from Sigma. Antibodies Used: ErbB3, Lamin A, Nrdp1 and a-Tubulin were from Cell Signaling Technology (Beverly, MA), AR and B-Actin were from Santa Cruz Biotechnology (Santa Cruz, CA) and FlnA was from Millipore (Billerica, MA).

Additional methods are described in Supplementary Materials

Plasmids: Human Nrdp1-luciferase constructs pGl4.11 ARE.03, mutated ARE.03, mutated right hand side ARE.03, and mutated left hand side ARE.03 were constructed as follows: A 500bp fragment immediately upstream of the Nrdp1 transcriptional start site was amplified from LNCAP genomic DNA using primers caTca gat Gcgc ggt acc GGT TAC GAA GCT CTG GGA TGC T and caTca gat Gcgc gct agc GAA GAC TCC TAC CAC TCG TCG C and then directionally cloned into the Kpn1 and Nhe1 cut pGL4.11 reporter construct (Promega). The ARE in the middle of this 500bp sequence was either left intact (Nrdp1 ARE.03 wild-type) or mutated at both half sites, or mutated individually within each ARE half-site.

PCR: The following primers were used; for PSA ARE with an annealing temperature of 58°C 5'-GCACGTGAGGCTTTGTATGA (forward) and 5-AAACCTTCATTCCCCAGGAC (reverse), Nrdp1

ARE.01 with an annealing temperature of 56.3°C 5'-ACCTCAGCTCATCTGCCTGT (forward) and 5'-AGGCAGGAGAAGCATTTGAA (reverse), Nrdp1 ARE.02 with an annealing temperature of 52°C 5'-CCTGTACTGGCTCCTCCAAGAC (forward) and 5'-TGAATGGATCTTGGCAATGAGT (reverse), and Nrdp1 ARE.03 with an annealing temperature of 56.3°C 5'-TTACGAAGCTCTGGGATGCT (forward) and 5'-CCCAGCCAGGACTATGTAGC (reverse)

***Mouse studies*:** 4-5-week old nu/nu athymic male mice were obtained from Harlan Sprague Dawley, Inc. (Indianapolis, IN) and implanted subcutaneously with sustained release testosterone pellets (12.5 mg, 90-day release; Innovative Research of America, Sarasota, FL). Suspensions of CWR22 cells were made in 50% Matrigel solubilized basement membrane (BD Biosciences, Bedford, MA) and xenografts were established by subcutaneous injections of 2.5×10^6 cells/site into both flanks. When palpable tumors were observed, animals were (i) left intact (sham operated: the animals were opened up, but then reclosed without any additional procedure) or (ii) castrated by bilateral orchiectomy in anesthetized mice. The animals were followed for approximately four weeks, after which the mice were euthanized, tumors were collected and divided into sections for paraffin-embedding.

Statistical analysis: Median staining levels were compared between cancer and non-cancer cells from the same subject using Wilcoxon signed-rank tests. Median staining levels were compared between levels of categorical demographic characteristics using Wilcoxon rank-sum tests, in the case of demographic characteristics with two levels, or using Kruskal-Wallis tests, in the case of demographic characteristics with more than 2 levels. The correlations between staining levels and continuous demographic characteristics were estimated using Spearmans' rho. All analyses were conducted using R, version 2.13.0 (R Development Core Team, 2011). Mice tumor data was analyzed by normalization of all measurements to pre-operation (sham or castration) measurements for each individual mouse, then mean and standard errors calculated for the aggregate group. For staining analysis, associations were based on Pearson's product moment correlation coefficient. Similar statistical considerations had been reported earlier in more details [21, 22].

RESULTS

Nrdp1 is expressed in both the nucleus and the cytoplasm of prostate epithelial cells. We previously showed that ErbB3 plays a major role in PCa progression and that ErbB3 levels are elevated during AWT due to suppression of the E3 ubiquitin ligase Nrdp1, which enables ErbB3 degradation [12]. Hence we investigated the expression of Nrdp1 in primary prostate tumor and surrounding non-tumor tissues available from the archives of the VA Northern California Health Care System (VANCHCS), Laboratory and Pathology Services. Sections from prostate tumors of 78 patients who underwent radical retropubic prostatectomy at VANCHCS between 1996 and 2002 were analyzed for these studies. Patient characteristics are described in **Supplementary Table 1.** The tissues were arranged in a tissue microarray (TMA) and sections of the TMA were stained with an antibody to Nrdp1. The specificity of the staining was verified in HEK 293T cells with a control or Nrdp1 shRNA **(Supplemental Figure 1).** In the prostate tissue, Nrdp1 was expressed in the nucleus, the cytoplasm or both, in various patients **(Figure 1A)**.

Both nuclear and cytoplasmic Nrdp1 levels in prostate tumor tissue correlate with nuclear AR expression. Using a Nrdp1 scoring system based on IHC intensity from 0 to 3, where 0 presents no Nrdp1 and 3 represents the highest protein levels, we observed that Nrdp1 nuclear protein levels remains consistent between tumor and non-tumor tissue, whereas cytoplasmic Nrdp1 was significantly increased in tumor tissue compared to non-tumor ($p<0.001$) **(Figure 1B, Supplementary Table 2)**. Examination of Oncomine datasets showed that a similar trend is observed in mRNA levels from human prostate as determined by various investigators; however, the same datasets also showed that AR levels were increased in tumor tissue vs non-tumor **(Supplementary Figure 2).** Hence, we also investigated the protein levels of AR in our TMA tissues **(Supplemental Figure 3)**. Comparison of AR and Nrdp1 levels revealed a significant correlation between Nrdp1 levels (both nuclear and cytoplasmic) and nuclear (active) AR (cytoplasmic: pairwise correlation coefficient: 0.42; $p<0.001$; nuclear: pairwise correlation coefficient: 0.26; $p=0.035$) **(Figure 1C, Supplementary Table 3)**. Hence

we postulated that Nrdp1 levels may be upregulated in prostate tumor in comparison with non-tumor tissue due to an increase in AR levels, perhaps in an attempt to suppress the levels of ErbB3.

Nrdp1 levels in the tumor tissues inversely correlated with PSA failure. Comparison of Nrdp1 expression in patients who later experienced PSA failure vs those whose cancer did not recur, showed that Nrdp1 staining in the nucleus of epithelial cells in the tumor regions was significantly lower in subjects with PSA failure, with a median staining level of 0.0 in subjects with PSA failure and a median staining level of 0.7 in subjects without PSA failure ($p = 0.029$) **(Figure 1D)**. Other demographic and baseline variables were not significantly associated with staining levels, however, the levels of cytoplasmic Nrdp1 was also considerably lower in patients with PSA failure **(Figure 1D)**. In logistic regression analysis of the probability of PSA failure by Nrdp1 levels in the nucleus of cancer cells, a trend was seen towards decreased probability of PSA failure with higher Nrdp1 levels ($p = 0.059$, odds ratio = 0.41, 95% CI = [0.15, 0.97]). The odds ratio here represents the incremental change in odds for each unit change in Nrdp1. The area under the ROC curve for Nrdp1 in the nucleus of cancer cells as a predictor of PSA failure is 0.604. These results indicate a trend towards lower Nrdp1 levels in more aggressive tumors, and a dependence on AR levels for expression.

Nrdp1 expression is androgen regulated. Since Nrdp1 expression is observed in both the nucleus and the cytoplasm in tumor tissue, we investigated the localization of this protein in androgen-dependent LNCaP PCa cells and a more aggressive subline C4-2, developed from recurrent LNCaP tumors in castrated nude mice [23]. In LNCaP cells, the protein was observed mostly in the cytoplasm while in C4-2 cells, it was observed mostly in the nucleus, (although some Nrdp1 expression was observed in both compartments in both lines) **(Figure 2A)**. Western blotting revealed that the cytoplasmic band in less aggressive LNCaP cells corresponded to a 36kDa band while the nuclear band in more aggressive C4-2 cells corresponded to a 28kDa band **(Figure 2B)**.

Nrdp1 is predicted to have multiple alternately spliced structures resulting in two major proteins isoforms of 317 amino acids (36kDa) and 246 amino acids (28kDa) **(Supplementary Figure 4A)**. In LNCaP cells, prolonged culture in medium containing CSS caused decreased expression of both the

36kDa and the 28kDa bands **(Figure 2C) (**see also **Supplementary Figure 4B** for the effect of prolonged exposure to CSS**)**. In contrast, addition of 1 nM dihydrotestosterone to cells cultured in the absence of androgens resulted in significant increase in Nrdp1 levels in the cytoplasm **(Figure 2D)**. These results show that Nrdp1 expression is androgen regulated.

AWT suppresses Nrdp1 levels in a mouse model of PCa progression. To confirm AR regulation of Nrdp1 *in vivo*, athymic nu/nu mice were subcutaneously implanted with CWR22 tumor cells and the xenografted mice were subjected to either castration (n=6) or a sham operation (n=6). Following castration the CWR22 tumors did not grow, while those that were sham operated continued to grow, indicating that the CWR22 tumors were androgen-dependent **(Figure 3A)**. At the end of the study, the tumors were collected, paraffin embedded, sectioned, and stained by immunohistochemistry (IHC). The levels of nuclear AR were significantly lower in castrated mice compared to the intact animals ($p=0.016$) while the cytoplasmic AR levels were higher **(Figure 3B),** indicating AR inactivation (AR is active in the nucleus). IHC on tumors samples to determine the levels of Nrdp1 demonstrated the presence of Ndrp1 in both the nucleus and the cytoplasm **(Figure 3C)**. The tumors were scored for the presence of Nrdp1 in the cytoplasm or the nucleus and showed no significant change in nuclear Nrdp1 but a strong decrease in cytoplasmic Nrdp1 after castration **(Figure 3D)**. Taken together with AR expression, these results demonstrate a correlation between nuclear AR and cytoplasmic Nrdp1, which showed a statistical correlation (Pearson correlation = 0.734) that was strongly significant ($p=0.0028$) **(Figure 3E, left)**. Because Nrdp1 was shown to regulate ErbB3 *in vitro* in PCa [12], we correlated ErbB3 levels with Nrdp1 in the intact mice and found a significant inverse relationship, (Pearson correlation = -0.533; $p=0.04$) **(Figure 3E, right)**. These results confirm our previous *in vitro* observation demonstrating that Nrdp1 levels are regulated positively by the AR and in turn, negatively regulate ErbB3 [12].

Comparison of CWR22 tumors to those formed from CRPC CWR22Rv1 cells (derived from castrated mice growing relapsed CWR22 tumors) showed that in both cases, cytoplasmic Nrdp1 staining was higher than that in the nucleus **(Supplementary Figure 5A)**. However, in contrast to

CWR22 tumors, CWR22Rv1 tumors did not demonstrate a significant change in Nrdp1 or AR expression after castration **(Supplementary Figure 5B)**. These results confirm androgen regulation of Nrdp1 in androgen-dependent PCa but not in CRPC.

Nrdp1 is a direct transcriptional target of the AR. Based on the above, we investigated whether Nrdp1 was a direct transcriptional target of AR. Nrdp1 is known to contain at least 5 promoter regions, which express three androgen response elements (ARE) **(Figure 4A)** – of these, ARE.01 and ARE.02 were located just upstream of the translated region, while ARE.03 was located 209 bp upstream of the transcriptional start site **(Supplementary Figure 4).** ARE.03 is a full 15-bp bipartite palindromic sequence very similar to the AREs found in PSA, the quintessential AR target gene, whereas ARE.01 and ARE.02 are non-palindromic half-sites **(Figure 4A, upper)**. Comparison of AR binding to the three ARE regions showed no significant difference in AR binding to ARE.01 **(Figure 4A, lower left)** or ARE.02 (not shown) among androgen-dependent and –independent cell lines, whereas AR binding to ARE.03 was higher in LNCaP cells (where Nrdp1 is androgen regulated), compared to that in LNCaP-AI cells (derived by continuous culture of LNCaP cells in CSS-containing medium), and in C4-2 cells (where Nrdp1 is independent of androgens) [12] **(Figure 4A, lower right)**. These results indicated that ARE.03 may be the more important mediator of AR regulation in *Nrdp1*.

To demonstrate androgen-responsiveness of AR binding to ARE.03, androgen-dependent LNCaP PCa cells were cultured in fetal bovine serum (FBS) containing high levels of androgens or in low androgen charcoal stripped FBS (CSS) [24], in the presence or absence of 1 nM DHT to stimulate AR transcriptional activity. In LNCaP cells the regulation of Nrdp1 is androgen-dependent, with a decrease of protein levels in CSS medium compared to FBS medium and a restoration of Nrdp1 protein levels in CSS with DHT added **(Figure 4B, left)**. In contrast, in C4-2 cells, AR binding to ARE.03 was weak, whereas that to the PSA promoter was strong **(Figure 4B, right)**. To test the potential responsiveness to AR, we created luciferase constructs with the Nrdp1 promoter region containing ARE.01 or ARE.03. The plasmids were transfected into LNCaP cells which were further treated with DMSO, 1 nM DHT, or the AR antagonist bicalutamde (Casodex; 10μM). The response of LNCaP cells

to ARE.01 was very low compared to PSA ARE **(Figure 4C)**; however, the response to ARE.03 was much stronger. Two luciferase constructs for ARE.03 were used - one wild-type and one with several bases mutated to prevent AR binding. Significantly, AR transcriptional activity on the Nrdp1 promoter increased 3-fold after the addition of DHT ($p=0.046$) but this effect was prevented by bicalutamide ($p>0.05$). In contrast, there was little to no luciferase activity when transfected with the mutated ARE.03, indicating the bases mutated (containing the ARE) were needed for transcription of Nrdp1 **(Figure 4D)**. This confirmed that ARE.03 of *Nrdp1* is indeed a direct transcriptional target of the AR in LNCaP cells.

Sensitivity of AR transcriptional activity to AR inhibition correlated with localization of the cytoskeletal protein FlnA in the nucleus. To determine the cause behind the difference in binding pattern of AR to ARE.03 in LNCaP and C4-2 cells, we analyzed the genomic region of Nrdp1 in LNCaP and C4-2 cells and found no sequence variation between the gene sequence of the Nrdp1 promoter in these two cell lines indicating that the lack of AR binding was not due to a mutation in the Nrdp1 promoter **(Supplementary Figure 6)**. Hence, other causes were investigated to account for the difference in characteristics.

Previous reports from our lab had shown that nuclear expression of the actin-binding protein FlnA is lost in CRPC but that reintroduction of FlnA in the nucleus can sensitize CRPC cells to AWT [16, 17]. Hence we investigated whether FlnA may restore the ability of AR in CRPC lines to regulate Nrdp1 transcription. In LNCaP cells, FlnA expression is strongly nuclear, whereas in C4-2 cells, it is strongly cytoplasmic. Transfection of a plasmid expressing C-terminal FlnA (FlnA 16-24), which resulted in the appearance of a 90kDa FlnA fragment [17, 18], restored nuclear expression of FlnA in C4-2 cells **(Figure 5A, upper panels)**, whereas transfection of a plasmid expressing N-terminal FlnA (FlnA 1-15), which resulted in the appearance of a 170 kDa FlnA fragment, did not affect its localization (not shown). FlnA has been identified in the nucleolus as well [25], but despite decreased FlnA expression in the nucleoplasm of C4-2 cells **(Figure 5A, middle panels)**, it's expression in the nucleolus remained unchanged. In addition, transfection of FlnA 16-24 reduced cell numbers **(Figure**

5A, lower panel). Thus, LNCaP cells, in which the AR transcriptionally targets Nrdp1, has nuclear FlnA, whereas C4-2 cells, where Nrdp1 is not significantly AR regulated, expresses cytoplasmic FlnA.

Based on the above, we investigated whether FlnA regulates AR transcriptional activity and whether restoration of FlnA nuclear localization promoted AR binding to its transcripitional targets. Since PSA is the most common AR transcriptional target, we first determined the effect of FlnA on PSA. Bicalutamide significantly inhibited AR transcriptional activity on a PSA promoter (67.8% decrease in AR activity induced by bicalutamide, $p=0.037$) in LNCaP cells subjected to control siRNA; however, upon FlnA downregulation using a FlnA siRNA **(Figure 5B, lower)**, the cells acquired resistance to bicalutamide **(Figure 5B, upper)**. Next, we investigated which domain of FlnA regulated AR activity on the same PSA promoter. When transfected with a control vector, LNCaP cells cultured in CSS experienced 72% inhibition of AR activity on PSA vs. FBS ($p<0.00001$), whereas transfection of FlnA 1-15, prevented this effect. In contrast, transfection with FlnA 16-24 increased the difference (80.24% change FBS vs CSS, $p=0.0002$) **(Figure 5C)**. Therefore, expression of N-terminal FlnA (FlnA 1-15), which remains cytoplasmic, prevented androgen responsiveness; while expression of C-terminal FlnA, which migrated to the nucleus, had the reverse effect. We conclude that the expression of nuclear FlnA imparted androgen sensitivity whereas in the absence of nuclear FlnA, AR continuously stimulated PSA in an androgen-independent manner.

The ability of the AR to regulate Nrdp1 levels correlates with the expression of 90kDa FlnA. In order to demonstrate correlation between FlnA expression and Nrdp1 control by AR in PCa, we utilized two cell lines derived from relapsed CWR22 tumors, CWR22Rv1 and CWR-R1. We previously showed that CWR22Rv1 cells do not express nuclear FlnA compared to the parental androgen-dependent line CWR22, which does so (see Supplemental material to [17]). Both cell lines are castration-resistant; however, CWR-R1 cells exhibited greater androgen sensitivity as demonstrated by the response of these cells to bicalutamide **(Figure 6A)**. Both lines express similar levels of AR ($p>0.05$), however, CWR-R1 cells expressed higher levels of FlnA compared to CWR22Rv1 ($p<0.01$) **(Figure 6B)**. Comparison by Western blotting indicated higher protein levels of FlnA in CWR-R1 in support of the increased mRNA levels, and the presence of AR in both lines, although Rv1 cells expressed higher

levels of a truncated form of AR, and lower levels of the full-length protein compared to R1, as we had previously shown [26] **(Figure 6C, left)**. ChIP assay showed AR binding to PSA ARE in both cell lines, but AR binding to Nrdp1 ARE.03 only in CWR-R1 cells which expressed nuclear 90kDa FlnA, but not CWR22Rv1 cells which expressed little FlnA **(Figure 6C)**. As a result, in CWR-R1 cells, Nrdp1 protein levels decreased in the absence of androgens but was restored upon addition of DHT, whereas in CWR22Rv1 cells, there was no correlation between androgen levels and Nrdp1 expression **(Figure 6D)**. Correspondingly, AR expression was also regulated in CWR-R1 cells in an androgen-dependent manner, whereas in CWR22Rv1 cells, where the major form of AR was the truncated form lacking the ligand binding domain, AR expression was ligand-independent. The levels of ErbB3 correlated negatively with Nrdp1 and hence in CWR-R1 cells, it was androgen-regulated, but not in CWR22Rv1. Taken together with results from the previous figure, we conclude that AR transcriptional regulation of Nrdp1, but not PSA, correlates with the expression of FlnA in the nucleus.

Ectopic expression of nuclear FlnA restores AR regulation of Nrdp1 in CRPC cells lacking inherent nuclear FlnA expression. Previous studies showed that nuclear FlnA interacts with the AR and acts as a co-regulator for transcriptional control [18, 27]. Therefore, we investigated whether FlnA nuclear localization regulated the ability of AR to bind to the Nrdp1 promoter and coordinate its transcription. As before, the AR failed to bind to Nrdp1 ARE.03 in C4-2 cells, however, transfection of FlnA 16-24 in C4-2 cells, which we have shown earlier to restore nuclear FlnA in C4-2 cells **(Figure 5A)**, reestablished AR binding to Nrdp1 ARE.03 **(Figure 7A)**. In order to determine if this reflected a renewal of AR transcriptional activity on Nrdp1 in C4-2 cells we also performed a luciferase assay on the C4-2 FlnA 16-24 cells using the Nrdp1 ARE.03 luciferase construct and the mutant ARE.03 construct. The cells were transfected with either vector and treated with DMSO, DHT, or bicalutamide. The mutant ARE.03 construct showed little AR transcriptional activity, while in cells transfected with the wild-type ARE.03 vector, transcription of the plasmid was increased in the presence of DHT and inhibited by bicalutamide, indicating a restoration of androgen-sensitivity **(Figure 7B)**. In contrast, other FlnA constructs that did not restore nuclear FlnA localization [17], did not have as significant an effect on Nrdp1 transcription. **(Figure 7C)**. Correspondingly, transfection of FlnA16-24 restored the

expression of cytoplasmic FlnA in C4-2 cells **(Figure 7D)**. We conclude that in androgen-dependent PCa, the AR is able to bind to the Nrdp1 ARE.03 region and cause transcription of Nrdp1 to downregulate ErbB3. After androgen ablation, the AR is no longer able to bind and prevents Nrdp1 transcription, which allows ErbB3 to be overexpressed **(Supplementary Figure 7)**. These results indicate that FlnA 16-24 is crucial for AR regulation of Nrdp1 in PCa and that introduction of nuclear FlnA can restore androgen regulation of Nrdp1.

DISCUSSION

Similar to androgen-dependent prostate cells, CRPC cells also rely on the AR for growth and survival [9]. The AR normally is activated by androgen binding, in CRPC, the requirement for androgens is abrogated and the AR can be activated by aberrant binding of non-specific ligands or in a completely ligand-independent manner. We previously showed that increased expression of ErbB3 promotes ligand-independent AR activation whereas the AR itself suppresses ErbB3 levels in androgen-dependent but not in CRPC cells [12]. AR regulation of ErbB3 is mediated by transcriptional regulation of Nrdp1 in androgen-dependent cells, but the AR loses the ability to target Nrdp1 in CRPC [12]. Here, we investigate the cause of this loss of AR function and mechanisms by which this function may be restored.

In this paper, we demonstrate that *Nrdp1* is a direct transcriptional target of the AR in androgen-dependent but not in CRPC cells. We previously showed that the AR also promotes the cleavage of a structural cytoplasmic protein, the 280kDa FlnA, to a 90kDa fragment that translocates to the nucleus [19]. Here, we show that restoration of FlnA to the nucleus promotes AR binding to the *Nrdp1*promoter, while making AR binding to the *PSA* promoter ligand-dependent. Our data indicate that FlnA helps redirect the AR and choose its targets. It is likely that AR binding to the *PSA* promoter is more indiscriminate compared to the requirements for it to bind the *Nrdp1* promoter. Future studies will determine whether FlnA helps recruit certain co-regulators that allow the AR to bind to the *Nrdp1* promoter whereas the same co-regulators are not required for *PSA* transcription.

In recent times, multiple investigators have compared the transcription programs the AR regulates in androgen-dependent vs castration-resistant cells [20, 28, 29]. These studies demonstrate that AR persistently occupies a distinct set of genomic loci after androgen deprivation in CRPC [28]. These androgen-independent AR occupied regions have constitutively open chromatin structures that lack the canonical androgen response element and are independent of FoxA1, a transcription factor involved in ligand-dependent AR targeting. In CRPC cells that express a truncated AR distinct from the full-length receptor, this may be accounted for as distinct transcription programs regulated by the two

AR isoforms [29]. For example, it was shown that the AR selectively upregulates M-phase cell-cycle genes in androgen-independent cells, unlike in androgen-dependent cells [20]. Our current results indicate that the presence of FlnA (and perhaps other similar proteins) in the nucleus likely contributes to this difference in program. The regulation of Nrdp1 is significant because of the implications in the effect of the AR on the activation of signaling pathways downstream of ErbB3, which has been implicated in the progression of several metastatic cancers including prostate cancer [12, 30].

Nrdp1 was first identified as a E3 ubiquitin ligase that caused ErbB3 degradation in breast cancer cells [14, 15, 30]. Since then, this RING finger containing molecule has been found to regulate other proteins as well, such as BRUCE, an inhibitor of apoptosis proteins (IAP) [31], parkin [32], the production of proinflammatory cytokines [33], type 1 cytokine receptor [34], and even transcription factor CCAAT/enhancer-binding Protein β (C/EBPβ) [35]; and may play a role in regulating ischemia and reperfusion-induced cardiac injury [36], differentiation of the melanocyte lineage [37], and sensitizes cells to oxidative stress [38]. A number of transcription factors other than AR may also have binding sites on the *Nrdp1* promoter, including SMAD, GATA3, FKHRL1, NANOG, OCT3/4, ER, VDR, E2F, CREB, EGR, STAT, PPARG, BARBIE and p53 (unpublished observations). On the other hand, other regulators of ErbB3 in PCa, such as Ebp1 [39], have been identified. Therefore, AR regulation of Nrdp1, or Nrdp1 regulation of ErbB3, is not absolute. However, our results indicate that Nrdp1 regulation of ErbB3 is an important mechanism by which the AR regulates the activation of escape mechanisms in PCa.

Our data indicate a function of Nrdp1 other than degradation of proteins. Two isoforms of Nrdp1 have been identified, a 36kDa and a 28kDa form. The 28kDa form lacks the RING finger domain and is therefore assumed to be a dominant negative form of the protein [40]. Here we show that the 28kDa form is primarily in the nucleus whereas the 36kDa form is primarily in the cytoplasm. Since the 36kDa form contains the RING finger domain and binds ErbB3 [14], which acts primarily in the plasma membrane, it will be active in the cytoplasm. On the other hand, the dominant negative form may be sequestered in the nucleus to prevent resistance to this process. However, ErbB3 is also present in the nucleus [41, 42]; it remains to be seen whether Nrdp1 interacts with ErbB3 in the nucleus as well. In

C4-2 cells, the 28kDa Nrdp1 isoform was the major isoform expressed and it was localized mostly in the nucleus; in these cells, the AR is unable to regulate Nrdp1 levels. Future studies will reveal whether androgen dependent transcription favors one form over the other.

This hypothesis explains why cytoplasmic, but not nuclear, Nrdp1 levels increase in tumor tissue compared to non-tumor prostate. Cytoplasmic Nrdp1 levels correlated with nuclear AR expression and hence in androgen-dependent PCa, an increase in AR levels stimulated Nrdp1 expression likely to prevent AR-independent signaling downstream of ErbB3, whereas androgen withdrawal relieves feedback inhibition which stimulates ErbB3 increase. On the other hand, Nrdp1 levels were significantly lower in tumors from patients who later undergo PSA failure. Multivariate analysis indicate that patients with lower Nrdp1 have a higher probability of undergoing PSA failure.

Finally, we demonstrate that the presence of nuclear FlnA determines the transcriptional target of the AR. AR binds ARE.03, but not ARE.01, on the proximal Nrdp1 promoter only in the presence of nuclear FlnA. Unlike Nrdp1, AR can bind to the proximal PSA promoter in the absence of nuclear FlnA; but in the presence of nuclear FlnA, AR binds to PSA ARE, similar to Nrdp1 ARE.03, in an androgen-dependent manner. Hence in the presence of nuclear FlnA, AR can bind its target gene (whether PSA or Nrdp1 ARE.03) only in the presence of androgens. However, in the absence of FlnA AR can still bind to PSA ARE, but not to Nrdp1. We conclude that in androgen-dependent cells expressing nuclear FlnA, in the presence of androgens, the AR transcribes Nrdp1 which suppress ErbB3 levels. Androgen withdrawal in these cells relieves feedback inhibition which promotes ErbB3 increase (leading to increased AR activity and elevated cell growth). However, in CRPC cells that lack FlnA nuclear localization, the AR is unable to bind to the Nrdp1 promoter, but binds to the PSA promoter, which results in increased PSA expression but does not prevent cell growth.

ACKNOWLEDGEMENTS

We thank Dr. Sheetal Singh, VA Northern California Health Care System, for comparing the nucleotide sequence of Nrdp1 ARE.03 in LNCaP and C4-2 cell lines. We also thank Ms. Stephanie Soares, Department of Urology, University of California Davis, School of Medicine, for the construction of the tissue microarrays used in this study. In addition, we thank the various investigators depositing microarray analyses data in public databases so that it can be accessed by laboratories all over the world. This work was supported by an Idea Development Award from the Department of Defense (PC081177, PMG), a Biomedical Laboratory Research & Development (BLRD) service Merit Award (I01BX000400, PMG) from the Department of Veterans Affairs and by Awards R01CA133209 (PMG), CA123541 (KLC) and GM068994 (KLC) from the National Institutes of Health.

REFERENCES

1. Catalona, W.J. (1994). Management of cancer of the prostate. N Engl J Med *331*, 996-1004.

2. Shapiro, D., and Tareen, B. (2012). Current and emerging treatments in the management of castration-resistant prostate cancer. Expert Rev Anticancer Ther *12*, 951-964.

3. Cheng, H., Snoek, R., Ghaidi, F., Cox, M.E., and Rennie, P.S. (2006). Short hairpin RNA knockdown of the androgen receptor attenuates ligand-independent activation and delays tumor progression. Cancer Res *66*, 10613-10620.

4. Seruga, B., and Tannock, I.F. (2011). Chemotherapy-based treatment for castration-resistant prostate cancer. J Clin Oncol *29*, 3686-3694.

5. Paller, C.J., and Antonarakis, E.S. (2012). Sipuleucel-T for the treatment of metastatic prostate cancer: promise and challenges. Hum Vaccin Immunother *8*, 509-519.

6. Pezaro, C.J., Mukherji, D., and De Bono, J.S. (2012). Abiraterone acetate: redefining hormone treatment for advanced prostate cancer. Drug Discov Today *17*, 221-226.

7. Ferraldeschi, R., Pezaro, C., Karavasilis, V., and de Bono, J. (2012). Abiraterone and Novel Antiandrogens: Overcoming Castration Resistance in Prostate Cancer. Annu Rev Med.

8. Rawlinson, A., Mohammed, A., Miller, M., and Kunkler, R. (2012). The role of enzalutamide in the treatment of castration-resistant prostate cancer. Future Oncol *8*, 1073-1081.

9. Yamaoka, M., Hara, T., and Kusaka, M. (2010). Overcoming persistent dependency on androgen signaling after progression to castration-resistant prostate cancer. Clin Cancer Res *16*, 4319-4324.

10. Carver, B.S., Chapinski, C., Wongvipat, J., Hieronymus, H., Chen, Y., Chandarlapaty, S., Arora, V.K., Le, C., Koutcher, J., Scher, H., Scardino, P.T., Rosen, N., and Sawyers, C.L. (2011).

Reciprocal Feedback Regulation of PI3K and Androgen Receptor Signaling in PTEN-Deficient Prostate Cancer. Cancer Cell *19*, 575-586.

11. Murillo, H., Huang, H., Schmidt, L.J., Smith, D.I., and Tindall, D.J. (2001). Role of PI3K signaling in survival and progression of LNCaP prostate cancer cells to the androgen refractory state. Endocrinology *142*, 4795-4805.

12. Chen, L., Siddiqui, S., Bose, S., Mooso, B., Asuncion, A., Bedolla, R.G., Vinall, R., Tepper, C.G., Gandour-Edwards, R., Shi, X., Lu, X.H., Siddiqui, J., Chinnaiyan, A.M., Mehra, R., Devere White, R.W., Carraway, K.L., 3rd, and Ghosh, P.M. (2010). Nrdp1-mediated regulation of ErbB3 expression by the androgen receptor in androgen-dependent but not castrate-resistant prostate cancer cells. Cancer Res *70*, 5994-6003.

13. Olayioye, M.A., Neve, R.M., Lane, H.A., and Hynes, N.E. (2000). The ErbB signaling network: receptor heterodimerization in development and cancer. Embo J *19*, 3159-3167.

14. Cao, Z., Wu, X., Yen, L., Sweeney, C., and Carraway, K.L., 3rd (2007). Neuregulin-induced ErbB3 downregulation is mediated by a protein stability cascade involving the E3 ubiquitin ligase Nrdp1. Mol Cell Biol *27*, 2180-2188.

15. Yen, L., Cao, Z., Wu, X., Ingalla, E.R., Baron, C., Young, L.J., Gregg, J.P., Cardiff, R.D., Borowsky, A.D., Sweeney, C., and Carraway, K.L., 3rd (2006). Loss of Nrdp1 enhances ErbB2/ErbB3-dependent breast tumor cell growth. Cancer Res *66*, 11279-11286.

16. Bedolla, R.G., Wang, Y., Asuncion, A., Chamie, K., Siddiqui, S., Mudryj, M.M., Prihoda, T.J., Siddiqui, J., Chinnaiyan, A.M., Mehra, R., de Vere White, R.W., and Ghosh, P.M. (2009). Nuclear versus cytoplasmic localization of filamin A in prostate cancer: immunohistochemical correlation with metastases. Clin Cancer Res *15*, 788-796.

17. Wang, Y., Kreisberg, J.I., Bedolla, R.G., Mikhailova, M., deVere White, R.W., and Ghosh, P.M. (2007). A 90 kDa fragment of filamin A promotes Casodex-induced growth inhibition in

Casodex-resistant androgen receptor positive C4-2 prostate cancer cells. Oncogene *26*, 6061-6070.

18. Loy, C.J., Sim, K.S., and Yong, E.L. (2003). Filamin-A fragment localizes to the nucleus to regulate androgen receptor and coactivator functions. Proc Natl Acad Sci U S A *100*, 4562-4567.

19. Mooso, B.A., Vinall, R.L., Tepper, C.G., Savoy, R.M., Cheung, J.P., Singh, S., Siddiqui, S., Wang, Y., Bedolla, R.G., Martinez, A., Mudryj, M., Kung, H.J., Devere White, R.W., and Ghosh, P.M. (2012). Enhancing the effectiveness of androgen deprivation in prostate cancer by inducing Filamin A nuclear localization. Endocr Relat Cancer.

20. Wang, Q., Li, W., Zhang, Y., Yuan, X., Xu, K., Yu, J., Chen, Z., Beroukhim, R., Wang, H., Lupien, M., Wu, T., Regan, M.M., Meyer, C.A., Carroll, J.S., Manrai, A.K., Janne, O.A., Balk, S.P., Mehra, R., Han, B., Chinnaiyan, A.M., Rubin, M.A., True, L., Fiorentino, M., Fiore, C., Loda, M., Kantoff, P.W., Liu, X.S., and Brown, M. (2009). Androgen receptor regulates a distinct transcription program in androgen-independent prostate cancer. Cell *138*, 245-256.

21. Bedolla, R., Prihoda, T.J., Kreisberg, J.I., Malik, S.N., Krishnegowda, N.K., Troyer, D.A., and Ghosh, P.M. (2007). Determining risk of biochemical recurrence in prostate cancer by immunohistochemical detection of PTEN expression and Akt activation. Clin Cancer Res *13*, 3860-3867.

22. Kreisberg, J.I., Malik, S.N., Prihoda, T.J., Bedolla, R.G., Troyer, D.A., Kreisberg, S., and Ghosh, P.M. (2004). Phosphorylation of Akt (Ser473) is an excellent predictor of poor clinical outcome in prostate cancer. Cancer Res *64*, 5232-5236.

23. Thalmann, G.N., Anezinis, P.E., Chang, S.M., Zhau, H.E., Kim, E.E., Hopwood, V.L., Pathak, S., von Eschenbach, A.C., and Chung, L.W. (1994). Androgen-independent cancer progression

and bone metastasis in the LNCaP model of human prostate cancer. Cancer Res *54*, 2577-2581.

24. Sedelaar, J.P., and Isaacs, J.T. (2009). Tissue culture media supplemented with 10% fetal calf serum contains a castrate level of testosterone. Prostate *69*, 1724-1729.

25. Deng, W., Lopez-Camacho, C., Tang, J.Y., Mendoza-Villanueva, D., Maya-Mendoza, A., Jackson, D.A., and Shore, P. (2012). Cytoskeletal protein filamin A is a nucleolar protein that suppresses ribosomal RNA gene transcription. Proc Natl Acad Sci U S A *109*, 1524-1529.

26. Chen, H., Libertini, S.J., Wang, Y., Kung, H.J., Ghosh, P., and Mudryj, M. (2010). ERK regulates calpain 2-induced androgen receptor proteolysis in CWR22 relapsed prostate tumor cell lines. J Biol Chem *285*, 2368-2374.

27. Ozanne, D.M., Brady, M.E., Cook, S., Gaughan, L., Neal, D.E., and Robson, C.N. (2000). Androgen receptor nuclear translocation is facilitated by the f-actin cross-linking protein filamin. Mol Endocrinol *14*, 1618-1626.

28. Decker, K.F., Zheng, D., He, Y., Bowman, T., Edwards, J.R., and Jia, L. (2012). Persistent androgen receptor-mediated transcription in castration-resistant prostate cancer under androgen-deprived conditions. Nucleic Acids Res.

29. Hu, R., Lu, C., Mostaghel, E.A., Yegnasubramanian, S., Gurel, M., Tannahill, C., Edwards, J., Isaacs, W.B., Nelson, P.S., Bluemn, E., Plymate, S.R., and Luo, J. (2012). Distinct transcriptional programs mediated by the ligand-dependent full-length androgen receptor and its splice variants in castration-resistant prostate cancer. Cancer Res *72*, 3457-3462.

30. Wu, X., Yen, L., Irwin, L., Sweeney, C., and Carraway, K.L., 3rd (2004). Stabilization of the E3 ubiquitin ligase Nrdp1 by the deubiquitinating enzyme USP8. Mol Cell Biol *24*, 7748-7757.

31. Qiu, X.B., Markant, S.L., Yuan, J., and Goldberg, A.L. (2004). Nrdp1-mediated degradation of the gigantic IAP, BRUCE, is a novel pathway for triggering apoptosis. EMBO J *23*, 800-810.

32. Zhong, L., Tan, Y., Zhou, A., Yu, Q., and Zhou, J. (2005). RING finger ubiquitin-protein isopeptide ligase Nrdp1/FLRF regulates parkin stability and activity. J Biol Chem *280*, 9425-9430.

33. Wang, C., Chen, T., Zhang, J., Yang, M., Li, N., Xu, X., and Cao, X. (2009). The E3 ubiquitin ligase Nrdp1 'preferentially' promotes TLR-mediated production of type I interferon. Nat Immunol *10*, 744-752.

34. Wauman, J., De Ceuninck, L., Vanderroost, N., Lievens, S., and Tavernier, J. (2011). RNF41 (Nrdp1) controls type 1 cytokine receptor degradation and ectodomain shedding. J Cell Sci *124*, 921-932.

35. Ye, S., Xu, H., Jin, J., Yang, M., Wang, C., Yu, Y., and Cao, X. (2012). The E3 ubiquitin ligase neuregulin receptor degradation protein 1 (Nrdp1) promotes M2 macrophage polarization by ubiquitinating and activating transcription factor CCAAT/enhancer-binding Protein beta (C/EBPbeta). J Biol Chem *287*, 26740-26748.

36. Zhang, Y., Zeng, Y., Wang, M., Tian, C., Ma, X., Chen, H., Fang, Q., Jia, L., Du, J., and Li, H. (2011). Cardiac-specific overexpression of E3 ligase Nrdp1 increases ischemia and reperfusion-induced cardiac injury. Basic Res Cardiol *106*, 371-383.

37. Maddirevula, S., Anuppalle, M., Huh, T.L., Kim, S.H., and Rhee, M. (2011). Nrdp1 governs differentiation of the melanocyte lineage via Erbb3b signaling in the zebrafish embryogenesis. Biochem Biophys Res Commun *409*, 454-458.

38. Zhou, A., Pan, D., Yang, X., and Zhou, J. (2011). Overexpression of Nrdp1/FLRF sensitizes cells to oxidative stress. Biochem Biophys Res Commun *410*, 771-774.

39. Zhou, H., Zhang, Y., and Hamburger, A.W. (2011). EBP1 inhibits translation of androgen receptor mRNA in castration resistant prostate cancer cells. Anticancer Res *31*, 3129-3135.

40. Diamonti, A.J., Guy, P.M., Ivanof, C., Wong, K., Sweeney, C., and Carraway, K.L., 3rd (2002). An RBCC protein implicated in maintenance of steady-state neuregulin receptor levels. Proc Natl Acad Sci U S A *99*, 2866-2871.

41. Koumakpayi, I.H., Diallo, J.S., Le Page, C., Lessard, L., Filali-Mouhim, A., Begin, L.R., Mes-Masson, A.M., and Saad, F. (2007). Low nuclear ErbB3 predicts biochemical recurrence in patients with prostate cancer. BJU Int *100*, 303-309.

42. Koumakpayi, I.H., Diallo, J.S., Le Page, C., Lessard, L., Gleave, M., Begin, L.R., Mes-Masson, A.M., and Saad, F. (2006). Expression and nuclear localization of ErbB3 in prostate cancer. Clin Cancer Res *12*, 2730-2737.

FIGURE LEGENDS

Figure 1. Nrdp1 levels in human prostate tumor tissue correlate positively with nuclear AR expression and negatively with PSA failure. (A). Formalin fixed paraffin-embedded human localized prostate cancer specimens obtained by prostatectomy were arranged in a tissue microarray and stained with anti-Nrdp1 antibody. Nrdp1 expression was observed in the nucleus, cytoplasm or both and was scored in both benign and cancerous prostate tissues. **(B).** Boxplots showing distribution of Nrdp1 and in the nucleus or cytoplasm of cancer compared to non-tumor tissue. The expression of nuclear Nrdp1 remains the same in both cancer and non-tumor tissues, whereas cytoplasmic expression of Nrdp1 increases in tumor compared to non-tumor tissue. **(C).** Boxplot showing correlation between levels of cytoplasmic Nrdp1 with nuclear AR ($p<0.001$). **(D).** Boxplot showing the decrease in Nrdp1 expression in patients who later underwent PSA failure compared to those who did not. Both nuclear and cytoplasmic levels of Nrdp1 decrease.

Figure 2. Nrdp1 isoforms are androgen regulated and differentially expressed in the nucleus and cytoplasm of androgen dependent and castration resistant prostate cancer cell lines. (A). (Top). Expression of Nrdp1 as determined by immunofluorescence in androgen-dependent LNCaP cells grown in FBS. Note that the majority of Nrdp1 in LNCaP cells is expressed in the cytoplasm**. (Bottom).** Expression of Nrdp1 as determined by immunofluorescence in CRPC C4-2 cells grown in FBS. Note that the majority of Nrdp1 in C4-2 cells is expressed in the nucleus**. (B).** Subcellular fractionation of LNCaP and C4-2 cells grown in CSS show that in LNCaP cells the 36kDa isoform of Nrdp1 is expressed mainly in the cytoplasm, with negligible levels of the 28 kDa isoform, while in C4-2 cells the 28kDa isoform is the dominating form and is mainly expressed in the nucleus (with a small amount of the 36 kDa isoform in the cytoplasm**. (C).** LNCaP cells were cultured in media containing FBS or CSS for 7 days. Cell lysates were immunoblotted with anti-Nrdp1 and anti-tubulin antibodies. Note that exposure to lower levels of androgens (CSS) caused a decrease in both 36 kDa and 28 kDa Nrdp1 levels**. (D). (Top).** Immunofluorescence of Nrdp1 in LNCaP cells grown in CSS showing loss of

Nrdp1 expression from the cytoplasm**. (Bottom).** Immunofluorescence of Nrdp1 in LNCaP cells in CSS media plus 1 nM DHT, showing that upon androgen stimulation, Nrdp1 levels in the cytoplasm increase.

Figure 3. Androgen withdrawal therapy (AWT) suppresses Nrdp1 levels in a mouse model of prostate cancer progression. (A). Nude mice were injected with CWR22 tumors and either castrated (n=6) or left intact (n=6). Tumor volume was measured periodically and expressed as mean ± Std error of volume normalized to day of castration. Note that tumor size in the intact mice increased by 3-fold within 29 days, whereas in the castrated mice they did not grow (max growth 1.2-fold after 10 days from day of castration) (p=0.02)**. (B).** Boxplot showing nuclear and cytoplasmic AR levels in the intact (sham-operated) and castrated mice bearing CWR22 xenografts. AR levels in the nucleus where significantly lower in the castrated group (mean score 1.03 ± 0.298) vs the intact group (mean score 1.55 ± 0.272) (p=0.0162), while AR levels in the cytoplasm were slightly higher in the castrated group (mean score 1.9 ± 0.2236) vs the intact group (mean score 1.38 ± 0.49) (p=0.0552). **(C).** Immunohistochemistry of CWR22 tumors from a castrated mouse **(right)**, and an intact mouse **(left),** demonstrating higher levels of cytoplasmic Nrdp1 in the intact mouse, but not nuclear Nrdp1, compared to castrated mice. **(D).** Boxplot showing nuclear and cytoplasmic Nrdp1 levels in the intact (sham-operated) and castrated mice bearing CWR22 xenografts. Nrdp1 levels in the nucleus where higher in the castrated group (mean score 1.0 ± 0.00) vs the intact group (mean score 0.78 ± 0.455) (p>0.05), while Nrdp1 levels in the cytoplasm were lower in the castrated group (mean score 0.9 ± 0.074) vs the intact group (mean score 1.14 ± 0.22) (p=0.05). **(E). (Left).** Comparison of AR vs cytoplasmic Nrdp1 levels in castrated CWR22 mice showing that as AR increases, so do cytoplasmic Nrdp1**. (Right).** Comparison of Nrdp1 vs ErbB3 levels in intact CWR22 mice showing that as Nrdp1 increases, ErbB3 levels decrease.

Figure 4. Nrdp1 is a direct transcriptional target of the androgen receptor. (A). (Top). Comparison of PSA and Nrdp1 AREs shows that the PSA ARE and Nrdp1 ARE.03 both contain a full

palondromic ARE, while ARE.01 and ARE.02 contain only a half site. **(Bottom).** ChIP assay of AR binding to Nrdp1 ARE.01 vs Nrdp1 ARE.03 in C4-2, LNCaP, and LNCaP AI. AR only binds to Nrdp1 ARE.03 in androgen dependent LNCaP cells and not androgen independent LNCaP AI and C4-2 cells **(right),** while it binds in all three cell lines to Nrdp1 ARE.01 **(left)**. Cells were cultured in FBS medium. Chromatin samples were immunoprecipitated with anti-AR antibody and analyzed by PCR with primers flanking the Nrdp1 ARE.03 and Nrpd1 ARE.01 regions. Input is control reactions of genomic DNA prior to immunoprecipitation. **(B). (Left).** ChIP assay of AR binding in LNCaP cells to ARE.03. Cells were cultured in FBS medium, CSS medium, or CSS medium with the addition of 1 nM DHT after the first day. Input is control reactions of genomic DNA prior to immunoprecipitation. Chromatin samples were immunoprecipitated with anti-AR andtibody and analyzed by PCR with primers flanking the Nrdp1 ARE.03 region**. (Right).** ChIP assay of AR binding in C4-2 cells to ARE.03 vs. PSA. Note that although AR did not bind to Nrdp1 ARE.03, it did bind to PSA in these cells. **(C).** AR binding to ARE.01 is not androgen-dependent. Luciferase assay was performed in cells transfected with a plasmid expressing ARE.01 or PSA. Compared to PSA, these cells activated very little Nrdp1 ARE.01. Cells were cultured in FBS medium and transfected with a control plasmid, a plasmid expressing PSA ARE, or Nrdp1 ARE.01 in the presence of DMSO, 1 nM DHT, or 10 μM bicalutamide, and AR transcriptional activity was measured by luciferase assay. **(D).** Mutation of normal ARE.03 to abolish AR binding**. (Top).** Nucleotide sequence of normal Nrdp1 ARE.03 and mutant ARE.03 that were inserted into luciferase constructs to test AR transcriptional activity. **(Bottom).** Increased AR transcriptional activity in LNCaP cells on wild-type and mutant ARE.03 in the presence of vehicle, 1 nM DHT or 10 μM bicalutamide (caso) compared with control vector and mutant ARE.03.

Figure 5. Sensitivity of AR transcriptional activity to AR inhibition correlated with localization of FlnA in the nucleus. (A). LNCaP, C4-2 and C4-2 cells stably transfected with FlnA 16-24 (C4-2 16-24) were stained by immunofluorescence for FlnA with an antibody specific to the C-terminus of FlnA. Immunofluorescent staining shows nuclear localization of FlnA in LNCaP cells (note the low level of FlnA in the cytoplasm) whereas in C4-2 cells FlnA was mainly localized to the cytoplasm but not in the

nucleoplasm, although bright staining in the nucleolus was also detected. In contrast, C4-2 16-24 cells expressed this protein equally in the cytoplasm and the nucleus, while nucleolar staining could still be detected. Middle panel demonstrates the individual cells highlighted in the upper panel. Lower panel demonstrates the cells in phase-contrast. **(B). (Top).** Luciferase assay in LNCaP cells to determine AR transcriptional activity on a PSA promoter tagged with a luciferase reporter. Data expressed has been normalized to corresponding expression of β-gal co-transfected as control. Cells subjected to control and FlnA siRNA were treated with vehicle (DMSO) or 10 μM bicalutamide for 48 hrs prior to the assay. Each point on the graph represents mean ± S.D. of 3 independent readings**. (Bottom).** Western blots to demonstrate the efficacy of the FlnA siRNA**. (C).** Luciferase assay in LNCaP cells to determine AR transcriptional activity on a PSA promoter to determine the effect of the N-terminal and C-terminal domains of FlnA on the AR 48 hrs after transient transfection. Cells were cultured in FBS vs CSS and collected after 48 hrs. Each point on the graph represents mean ± S.D. of 3 independent readings.

Figure 6. AR regulates Nrdp1 levels in cells expressing 90 kDa FlnA. (A). Androgen sensitivity in CWR-R1 vs. CWR22-Rv1 cells. The AR transcriptional activity was tested by inserting the PSA ARE into a luciferase construct. A decrease of luciferase activity in CWR-R1 cells, but not in CWR22-Rv1 cells, in the presence of 10 μM bicalutaide indicates that CWR-R1 cells are more androgen sensitive compared to CWR22Rv1 cells, even though they are both considered castration resistant (note that bicalutamide only decreased AR transcriptional activity on the PSA promoter by ~38%). **(B).** qPCR for AR and FlnA expression in CWR-R1 and CWR22-Rv1. Higher expression of FlnA was observed in CWR-R1 cells, although AR expression in the two cell lines was considered comparable. Results provided were normalized to the corresponding values for GAPDH. **(C). (Left).** CWR-R1 cells contain higher protein levels of full length and the 90kDa form of FlnA, compared to CWR22-Rv1 cells**. (Right).** ChIP assay of AR binding to ARE.03 in CWR-R1 and CWR22-Rv1 cells. Chromatin samples were immunoprecipitated with anti-AR andtibody and analyzed by PCR with primers flanking the Nrdp1 ARE.03 region and PSA ARE region. Input is control reactions of genomic DNA prior to immunoprecipitation**. (D).** Protein expression of ErbB3, Nrdp1, and AR in CWR-R1 and CWR22-Rv1

cutured in FBS, CSS or CSS with increasing doses of DHT as indicated. Cell lystaes were immunoblotted with anti-Nrdp1, anti-ErbB3, anti-AR, and anti-tubulin antibodies.

Figure 7. Nuclear Filamin A restores androgen receptor regulation of Nrdp1 in androgen independent cells. (A). AR binds to ARE.03 in in the presence of 90 kDa FlnA. ChIP assay of AR binding in LNCaP, LNCaP AI, C4-2, and C4-2 FlnA 16-24 cells. Chromatin samples were immunoprecipitated with anti-AR antibody and analyzed by PCR with primers flanking the Nrdp1 ARE.03 region. Input is control reactions of genomic DNA prior to immunoprecipitation. **(B).** AR transcriptional activity of Nrdp1 ARE.03 is androgen regulated in the presence of FlnA 16-24. Cells were cultured in FBS medium and transfected with the control vector, normal ARE.03, or mutant ARE.03, and AR transcriptional activity was measured by luceriferase assay. Cells were also treated with DMSO, DHT, or casodex. **(C).** FlnA restores AR transcriptional activity on Nrdp1 ARE.03 in androgen independent cells. Cells were cultured in FBS medium and transfected with full-length FlnA, FlnA repeats 1-15, or FlnA repeats 16-24, and AR transcriptional activity was measured by luceriferase assay. **(D). (Top).** Immunofluorescence of Nrdp1 in C4-2 cells showing Nrdp1 mostly in the nucleus. **(Middle).** Immunofluorescence of Nrdp1 in C4-2 cells transfected with pCMV-FlnA 1-15 showing Nrdp1 mostly in the nucleus**. (Bottom).** Immunofluorescence of Nrdp1 in C4-2 transfected with pCMV-FlnA 16-24, showing Nrdp1 goes to the cytoplasm in the presence of nuclear FlnA.

SUPPLEMENTARY MATERIAL

Loss of Androgen Receptor targeting of Nrdp1, a negative regulator of ErbB3, in castration resistant prostate cancer, and its reversal by Filamin A nuclear localization

SUPPLEMENTARY METHODS

Western blotting. Whole cell extracts were prepared by washing the cells twice in PBS and lysing cells in 250 µl cell lysis buffer (50 mM Tris HCl, pH 7.4, 150 mM NaCl, and 1% NP-40, and protease inhibitors: 0.1 mM benzamidine, 1 mM phenylmethylsulfonyl fluoride, 10 mg/ml each of phenathroline, leupeptin, aprotinin, and pepstatin A) and phosphatase inhibitors: 20 mM β-glycerol phosphate, 1 mM Na-orthovanadate, and 10 mM NaF. Proteins were quantitated using a BCA assay (Pierce, Rockford IL) and fractionated on 29:1 acrylamide-bis SDS-PAGE. Electrophoresis was performed at 150 V for 120 min using minivertical electrophoresis cells (Mini-PROTEAN 3 Electrophoresis Cell, Bio-Rad, Hercules, CA). The gels were electroblotted for 2 h at 200 mA using a Mini Trans-Blot Electrophoretic Transfer Cell (Bio-Rad) onto 0.2-µm polyvinylidene difluoride membrane (Osmonics, Westborough, MA). The blots were stained with primary antibodies at a dilution of 1:250 or 1:500. The staining was detected by enhanced chemiluminescence (Pierce) after incubation with a peroxidase-labeled secondary antibody (Donkey anti-mouse IgG, Chemicon, Temecula, CA, Goat anti-rabbit IgG, F_c specific, Jackson Immunoresearch, West Grove, PA).

MTT Assay: MTT cell proliferation was performed as shown previously [1, 2]. Cells were plated in 100mM dishes, transfected with vectors and then plated in 24-well plates. For collection, each well was incubated with 15 µl of 5 mg/ml 3-[4,5-Dimethylthiazol-2yl]v-2,5-diphenyl-tetrazolium bromide (MTT) (Sigma-Aldrich, St. Louis, MO) for 1 hour in a CO_2 incubator at 37^{o}C. Proliferation rates were estimated by colorimetric assay reading formazan intensity in a plate reader at 570 nm.

Mutagenesis was performed using the Stratagene QuikChangeII kit from Agilent technologies according to the manufacturer's instructions. Briefly, mutagenic primers were designed using the Agilent technologies QuikChange Primer Design program and were used to amplify nascent plasmid containing the desired mutation(s). Following PCR amplification the PCR reaction was digested with DpnI restriction enzyme to remove the parent plasmid and the remaining mutant plasmid was transformed into bacteria, followed by plasmid isolation. All mutant plasmids described were fully sequenced to confirm that their sequence was correct.

AR transcriptional activity: Reporter gene activity was determined by luciferase assay. LNCaP and/or C4-2, LNCaP AI, CWR22Rv1, CWR22R1 cells were transfected with 2 µg of pGL3-hPSA-luc and β-galactosidase with or without co-transfection of 2 µg of various FlnA vectors using Lipofectamine 2000 (Invitrogen, Grand Island, NY) according to the manufacturer's recommendations. Cells were treated as indicated for 72 hours. Cells were harvested 72 hours after transfection, and cell lysates prepared for performing luciferase assays using a luciferase enzyme assay system (Promega Corp., Madison, WI). Each transfection experiment was performed in triplicate. Results were normalized to β-galactosidase measured by a colorimentric assay and represent an average of 3 independent experiments with data presented as relative luciferase activity using means of untreated controls as standards.

Immunohistochemistry**:** Mouse tumors were fixed in 10% buffered formalin (Medical Industries, Richmond IL) for 30 mins at RT, after which the pellet was immersed in 600 µl liquefied agar at 50-60^{o}C. The agar containing the tumor was paraffin-embedded and processed based on established protocols. The paraffin-embedded cell block was then sectioned and sections were heated to 60^{o}C, and rehydrated in xylene and graded alcohols. Antigen retrieval was performed with 0.1M citrate buffer at pH 6.0 for 20 minutes in a 95% water bath. Slides were allowed to cool for another 20 minutes, followed by sequential rinsing in PBS and 50 mM Tris HCl, pH 7.6, 150 mM NaCl, Tween 20 (0.1%) (TBS-T). Endogenous peroxidase activity was quenched by incubation in TBS-T containing 3% hydrogen peroxide. Each incubation step was carried out at room temperature and was followed by three sequential washes (5 minutes each) in TBS-T. Sections were incubated in primary antibody diluted in TBS-T containing 1% ovalbumin and 1 mg/ml sodium azide (12 hours), followed by incubations with biotinylated secondary antibody for 15 minutes, peroxidase-labeled streptavidin for 15 minutes (LSAB-2 Dako Corp, Carpenteria CA) and diaminobenzidine and hydrogen peroxide chromogen substrate (Dako Corp.

Carpentaria CA) along with DAB enhancer (Signet) for 10 minutes. Slides were counter-stained with hematoxylin and mounted. Negative controls were incubated with the same amount of antihuman polyclonal rabbit IgG in place of primary antibody.

Chromatin Immunoprecipitation: Chip studies were conducted as previously described [3] with the following modifications: Chromatin was sonicated to an average size of 200 to 800 bp from 4.5 X 10^7 cells using Sonicator Ultrasonic Processor model S-4000. Sonicated chromatin was diluted 1:3 in dilution buffer (0.01% SDS, 1.1% Triton X-100, 1.2 mM EDTA, 16.7 mM Tris-Cl pH 8.0, 167 mM NaCl and a protease inhibitor cocktail (Sigma)). 1.5 µg of normal rabbit IgG (Santa Cruz Biotechnology) was added for 1.5 hr at 4 degrees Celsius and pulled down with 20 µl of Protein G Agarose/Salmon Sperm DNA beads (Millipore Billerica, MA) at room temperature to preclear. The precleared chromatin was split in two. 1.5 µg of AR (N-20) and normal rabbit IgG (Santa Cruz Biotechnology) were added to separate aliquots. Following cleanup, the samples were run on a 1% agarose gel and the region between 200 to 500 bp was cut out and purified using the QIAquick gel extraction kit (Qiagen, Inc.).

qPCR: Total cellular RNA was prepared utilizing RNeasy mini kit (Qiagen, Inc. CA) based on the manufacturer's protocol. cDNA was synthesized from 1 mg RNA using Marligen First Strand cDNA Synthesis Kits (Marligen, Rockville, MD) based on the manufacturer's protocol. Real-time PCR was run using TaqMan Gene Expression Master Mix (Applied Biosystems, Grand Island, NY) according to manufacturer's recommendations. B-Actin was used as the endogenous expression standard. Assays used were ID # B-Actin: 4333762T Filamin A: Hs00155065_m1 and Androgen Receptor: Hs00907244_m1 from Applied Biosystems (Grand Island, NY). Data was collected on an Applied Biosysytems 7500 Fast machine and analyzed using the relative standard curve method.

Program- The detection of the immunoprecipitated AR binding sites was done by PCR. For each sample (input, IgG, or androgen receptor) .1uL GoTaq polymerase (Promega), 4µl 5X GoTaq Buffer, .4µl 10uM F Primer, .4µl 10uM R Primer, .4µl 10µM dNTPs, 2µl DN, and 12.7µl ddH2O were mixed for PCR amplification in a 20µL reaction volume. The PCR was started with an initial denaturation of 95°C for 3 min, next 33 cycles of denaturation at 95°C for 30 sec, annealing at X°C for 15 sec, and extension step at 72°C for 15 sec, and lastly second extension step of 72°C for 4 min. The PCR products were separated on a 2% agarose gel and visualized by ethidium bromide staining.

Subcellular fractionation: Cells were plated in a 100 mm dish and grown to 70% confluence. They were then treated as described and separated into cytoplasmic and nuclear fractions as follows: the plates were washed with PBS twice and the cells collected in 0.5 ml of Buffer A (10 mM HEPES, pH 7.9, 10 mM KCl, 0.1 mM EDTA, 0.5 mM DTT) containing 200 µl of 10% IGEPAL and protease inhibitors (0.1 mM benzamidine, 1 mM PMSF, 10 µg/ml each phenathroline, leupeptin, aprotinin, and pepstatin A). Following 10 min incubation at room temperature, the lysate was transferred to ice and centrifuged at 4°C at 1500 rpm in a benchtop refrigerated centrifuge (Eppendorf 5417R) for 5 min, and the supernatant collected as the cytosolic fraction. The pellet containing the nuclei was resuspended in 150 ml of Buffer B (20 mM HEPES, pH 7.9, 0.4M NaCl, 1 mM EDTA, 10% Glycerol) containing the same protease inhibitors and solubilized by vigorous shaking at 4°C for 2h. The suspension was then centrifuged at 4°C as before for 5 min and the supernatant collected as the nuclear fraction.

Immunofluorescence: C4-2 cells were transfected with either pCMV-empty vector, pCMV-FlnA 1-15, or pCMV-FlnA 16-24 and seeded at 30,000 cells per coverslip and LNCaP cells were seeded at 60,000 cells per coverslip and were incubated for 24hrs in FBS medium in a 37^0C CO_2 incubator. They were then grown in either FBS, CSS, or CSS with 1nM DHT. The cells were then incubated for 48 hrs in the 37^0C CO_2 incubator. The cells were then rinsed with PBST (Phosphate Buffered Saline with 0.05% Tween-20) and then fixed with ice cold methanol for 10 min at room temperature. They were washed three times with PBST and then blocked with 10% BSA for 30 min at room temperature. Primary antibody, prepared in 1% BSA was applied to the cells and cells were incubated at 4^oC overnight. Cells were washed three times with PBST and the FITC conjugated anti-rabbit secondary antibody (Jackson Immuno Research) was diluted 1:200 in 1% BSA and incubated for 30 min at room temperature in the dark. After washing three times with PBST, slow fade mounting medium with DAPI (Invitrogen, Carlsbad, CA) was applied to the slides and the cover slips were mounted.

SUPPLEMENTARY DATA

Spplementary Table 1. Patient Characteristics.

Characteristics for 78 patients with primary prostate cancer, who underwent radical retropubic prostatectomy between 1999-2002,that were selected for the study. The patients were selected based on (i) availability of patient outcome data and (ii) availability of tissues from prostatectomy specimen.

Supplementary Figure 1. Nrdp1 Antibody Characterization. Antibody Characterization of US Biologicals Nrdp1 Antibody.

293T HEK cells were transfected with control or Nrdp1 shRNA to show the specificity of a rabbit polyclonal anti-Nrdp1 antibody (US Biologicals).

A. Western blot analysis showed Nrdp1 staining as a non-specific 65 KDa and a specific 36 KDa bands. Specificity of the lower band was determined by knockdown of Nrdp1 upon shRNA use, and a corresponding increase of p-ErbB3. 293T HEK cells were grown in FBS media. Cell lystaes were immunoblotted with andti-Nrdp1, anti-p-Erb3 and anti-tubulin antibodies.
B. 293T HEK cell pellets (similarly treated) were paraffin embedded, sectioned and stained with the same Nrdp1 antibody. Lack of background staining in the shRNA-treated cells denotes that the IHC staining was more specific.

Supplementary Table 2. Protein Staining in Cancer and Non-Cancer Cells

Comparison of Nrdp1 and AR in a cytoplasmic or nuclear location in cancer vs. non-cancer cells. Cytoplasmic but not nuclear AR and Nrdp1 expression increase in human prostate tumor tissues compared to non-tumor prostate. P-value ($p<0.05$) were considered significant. Numerical values for boxplot of Figure 1B and Suppletmentary Figure 3.

Supplementary Figure 2. AR and Nrdp1 expression in cancer and normal cells.

Confirmation of the up regulation of Nrdp1 and AR in cancer vs. normal and the correlation between the three Oncomine datasets. (For AR, p = 3.26 x 10^-8; for NRDP1, p = 1.62 x 10^-6; values calculated using Fisher's combined probability test). Box plots shown are from studies in the Oncomine database representative of overall trend.

Supplementary Figure 3. AR Staining in Cancer and Normal Cells.

Boxplots showing distribution of AR in the nucleus and cytoplasm of cancer tissue compared to non-tumor tissue. The expression of nuclear AR and remains the same in both cancer and non-tumor tissues, whereas cytoplasmic expression increases in cancer.

Supplementary Table 3. Pairwise Correlations Between Staining Factors in Cancer Cells.

Nuclear and cytoplasmic comparison of AR and Nrdp1. Correlation between Nrdp1 and AR in cancer cells. Strongly significant correlations were found between nuclear AR and cytoplasmic Nrdp1. Numerical values of boxplot of Figure 1C.

Supplementary Figure 4. Increase of nuclear Nrdp1 in castration resistant mouse tumors.

A. Boxplot of Nrdp1 nuclear and cytoplasmic expression levels in CWR22Rv1 mice vs. CWR22 mice, both showing higher Nrdp1 levels in the cytoplasm vs. the nucleus.
B. Boxplot showing Nrdp1 nuclear and cytoplasmic levels in the castrated and non-castrated CWR22Rv1 mice. Nrdp1 levels in the nucleus remain constant after castration, but decrease in the cytoplasm.
C. Boxplot showing AR nuclear and cytoplasmic levels in the castrated and non-castrated CWR22Rv1 mice. AR levels in the nucleus and the cytoplasm remain consistent in both after castration, indicating that the androgen receptor is androgen independent.
D. Comparison of AR levels and Nrdp1 levels in CWR22Rv1 mice showing that as nuclear AR increases, so do nuclear Nrdp1 levels.

Supplementary Figure 5. Protein structure of 36 kDa and 28 kDa Nrdp1 forms.

Top. mRNA transcript and protein structure of the 36kDa form of Nrdp1.

Bottom. mRNA transcript and protein structure of the 28kDa form of Nrdp1.

The mRNA transcripts show the location of ARE.03 and ARE.01 in the Nrdp1 transcripts, translational stop site, and difference in the translational start site between the two isoforms. The protein structures are the same for the C-terminal end, including the 2nd peroximal domain, the coiled coil, and the USP8 interacting domain, while only the 36kDa protein contains two U-box domains and the Zinc (RING) finger domain.

Supplementary Figure 6. Differential expression of Nrdp1.

A. Nrdp1 levels correspond with the addition of DHT. LNCaP cells were cultured in FBS or CSS medium in the presence or absence of DHT after the first day. Cell lysates were immunoblotted with anti-Nrdp1 and

anti-tubulin antibodies. In CSS media and the absence of DHT Nrdp1 expression levels go down compared its expression levels in FBS media or in CSS media supplemented with DHT. This also corresponds to AR binding to ARE.03.

B. Nrdp1 protein levels correspond with androgen dependence. C4-2 and LNCaP cells were grown in FBS medium. Cell lystaes were immunoblotted with andti-Nrdp1 and anti-tubulin antibodies. In LNCaP cells, where AR binds to Nrdp1 ARE.03, there is a high level of Nrdp1 expression compared to in C4-2 cells, where AR does not bind to Nrdp1 ARE.03

Supplementary Figure 7. Nrdp1 ARE.03 Genomic Sequence

Nucleotide comparison of the Nrdp1 ARE.03 sequence in LNCaP and C4-2 showing no mutation in the sequence despite a change in AR binding in the two cell lines.

Supplementary Figure 8. AR control of Nrdp1 in castration sensitive vs. castration resistant prostate cancer cells.

In castration sensitive tumors, the androgen receptor is regulated by the presence of nuclear FlnA. This allows androgen receptor to bind to the ARE upstream of the Nrdp1 gene, ARE.03, and cause an increase of Nrdp1 expression. This in turn down regulates ErbB3 and prevents cell growth. In castration resistant tumors, nuclear FlnA is no longer present, which causes aberrant binding and androgen receptor no longer binds to ARE.03, preventing Nrdp1 expression. This then allows ErbB3 protein levels to increase and causes increased cell growth.

SUPPLEMENTAL REFERENCES

1. Ghosh, P.M., N. Ghosh-Choudhury, M.L. Moyer, et al., *Role of RhoA activation in the growth and morphology of a murine prostate tumor cell line.* Oncogene, 1999. **18**(28): p. 4120-30.
2. Ghosh, P.M., S.N. Malik, R.G. Bedolla, et al., *Signal transduction pathways in androgen-dependent and -independent prostate cancer cell proliferation.* Endocr Relat Cancer, 2005. **12**(1): p. 119-34.
3. Weinmann, A.S., S.M. Bartley, T. Zhang, et al., *Use of chromatin immunoprecipitation to clone novel E2F target promoters.* Mol Cell Biol, 2001. **21**(20): p. 6820-32.

http://www.genecards.org/cgi-bin/carddisp.pl?gene=RNF41
http://uswest.ensembl.org/Homo_sapiens/Gene/Splice?g=ENSG00000181852;r=12:56598285-56615737;redirect=mirror;source=www.ensembl.org

Supplementary Data

Androgen Receptor targeting of Nrdp1, a negative regulator of ErbB3, restored by Filamin A nuclear localization in castration resistant prostate cancer

Patient Characteristics

Number of patients		78
RACE	Caucasian	38
	African American	17
	Others	23
Mean BMI		28.47 ± 4.48
Mean Pre-op PSA		7.99 ± 6.48
GLEASON	Gleason 5-6	35
	Gleason 7	33
	Gleason 8-9	9
STAGE	STAGE T1	43
	STAGE T2	35
POSITIVE MARGINS		27
PSA FAILURE		23

SUPPLEMENTARY TABLE 1

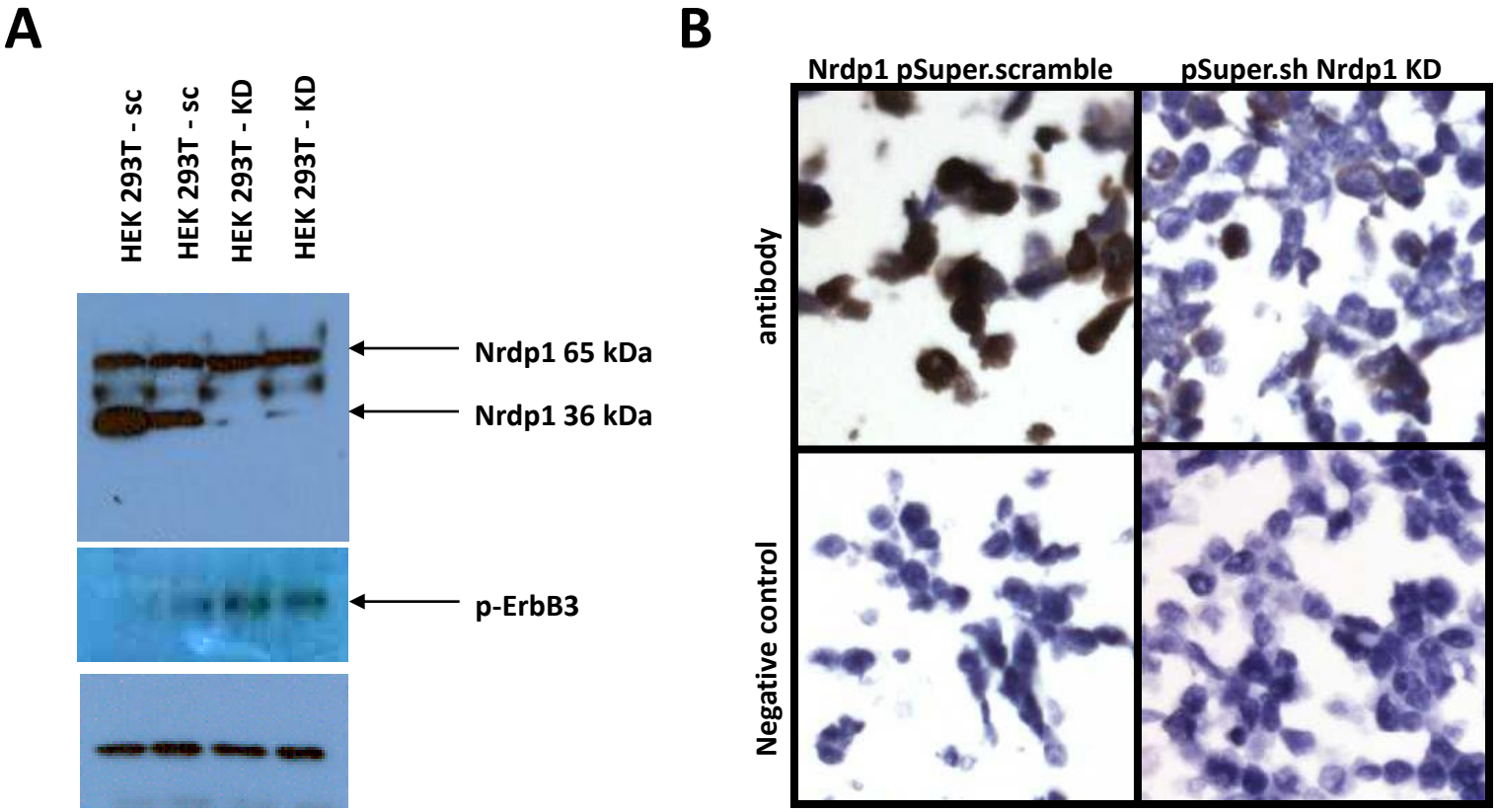

SUPPLEMENTARY FIGURE 1

Nrdp1 and AR staining in localized prostate tumor and corresponding non-tumor tissue

Supplementary Table 2: Staining in Cancer and Non-Cancer Cells						
	Cytoplasm			**Nucleus**		
Protein	Median in Cancer Cells	Median in Non-Cancer Cells	P-Value (Wilcoxon Signed Rank Test)	Median in Cancer Cells	Median in Non-Cancer Cells	P-Value (Wilcoxon Signed Rank Test)
Nrdp1	1.0	0.5	<0.001	0.3	0.3	0.134
AR	1.0	0.8	<0.001	2.0	2.0	0.071

Legend
1. Prostate Gland
2. Prostate Carcinoma

SUPPLEMENTARY FIGURE 2

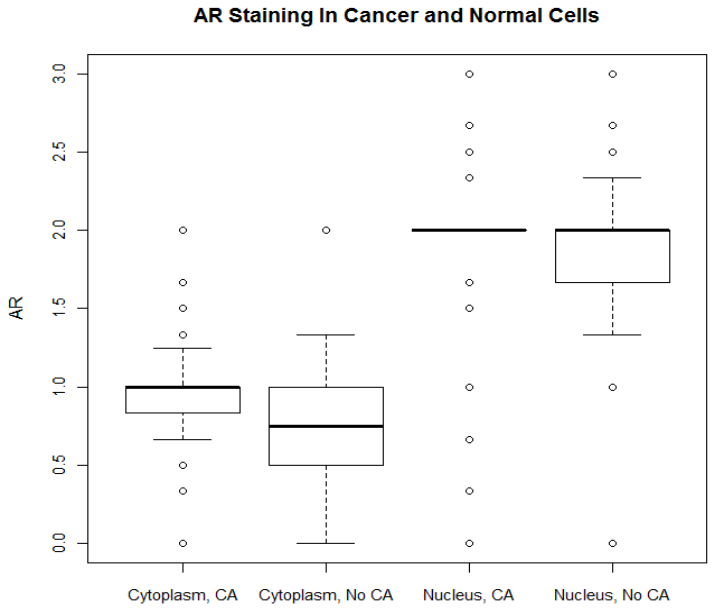

SUPPLEMENTARY FIGURE 3

Pairwise Correlations Between Nrdp1 and AR Staining in Prostate Cancer

Supplementary Table 3: Pairwise Correlations Between Staining Factors in Cancer Cells				
Spearman's Rho (P-Value)	Nrdp1 Nucleus	Nrdp1 Cytoplasm	AR Nucleus	AR Cytoplasm
Nrdp1 Nucleus		**0.6 (<0.001)**	**0.26 (0.035)**	**0.27 (0.026)**
Nrdp1 Cytoplasm	**0.6 (<0.001)**		**0.42 (<0.001)**	0.23 (0.058)
AR Nucleus	**0.26 (0.035)**	**0.42 (<0.001)**		0.06 (0.617)
AR Cytoplasm	**0.27 (0.026)**	0.23 (0.058)	0.06 (0.617)	

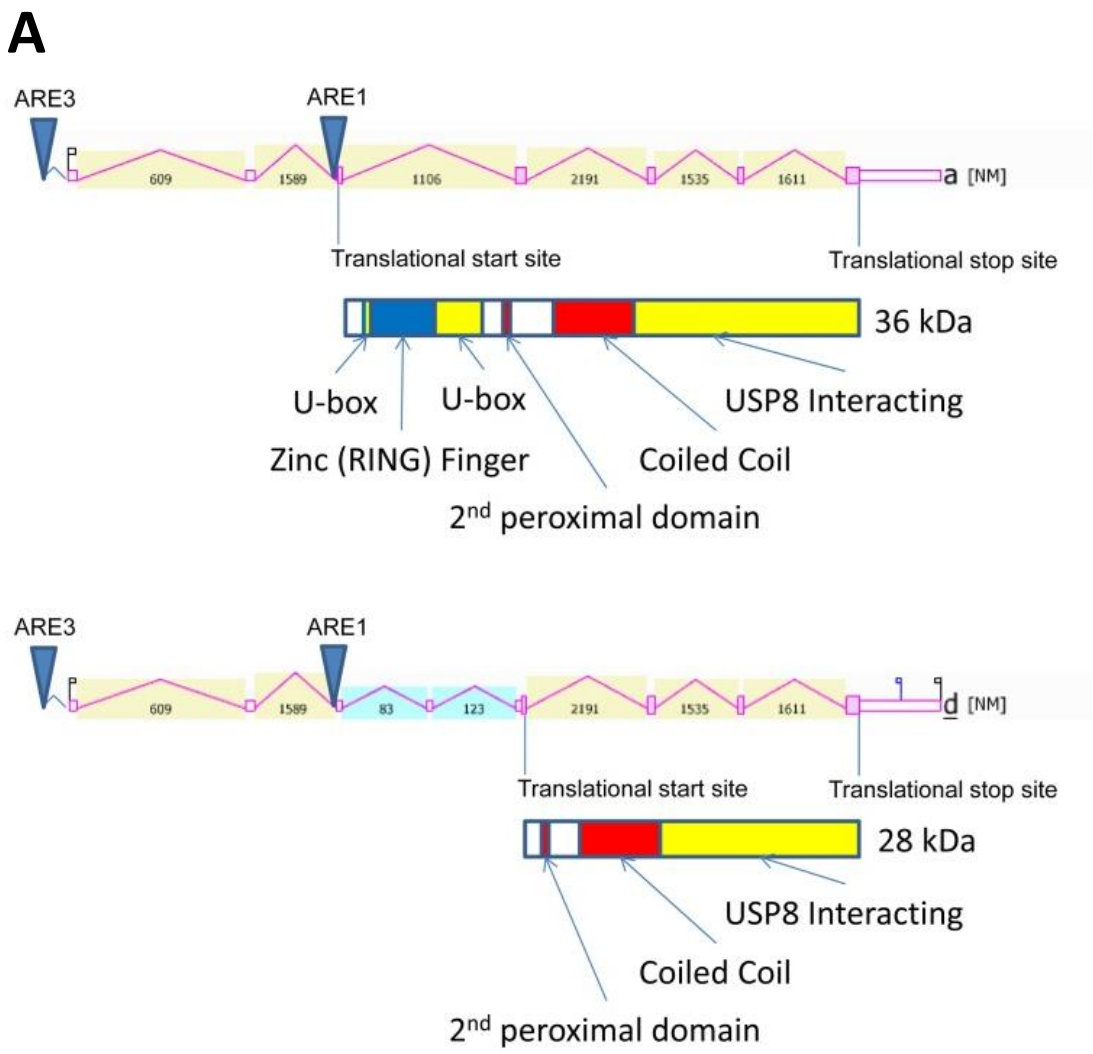

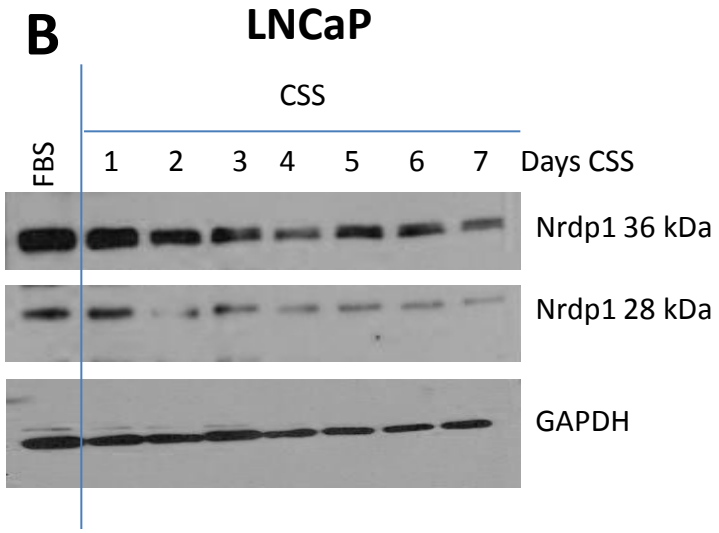

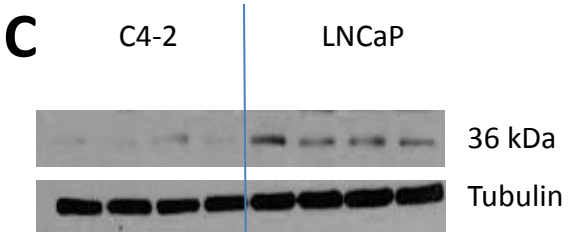

SUPPLEMENTARY FIGURE 4

A

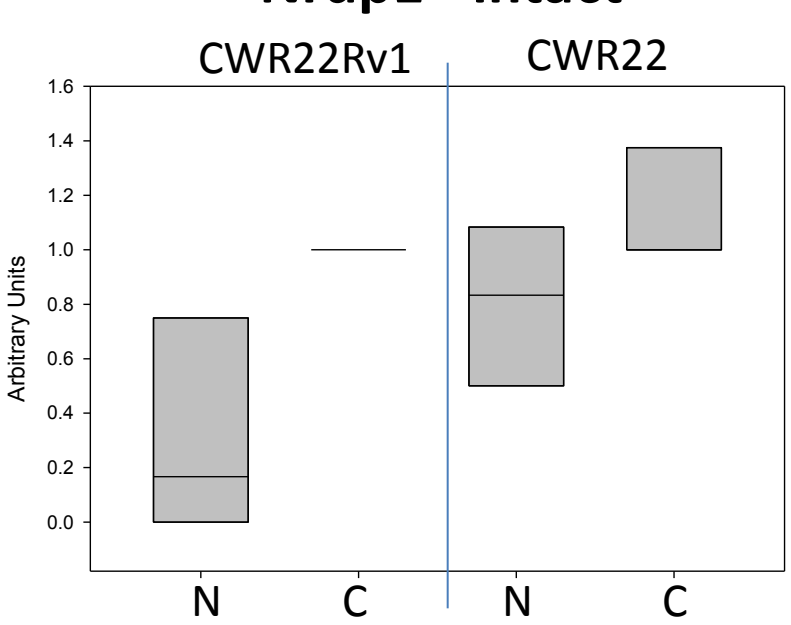

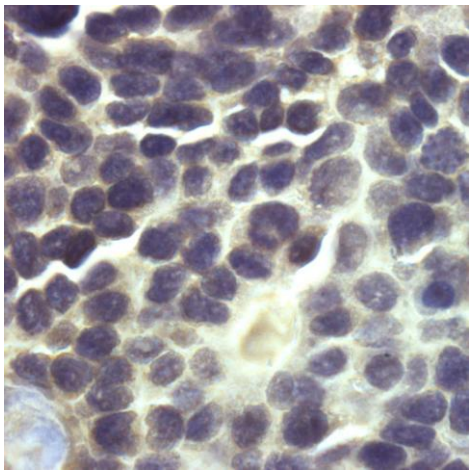

CWR22Rv1

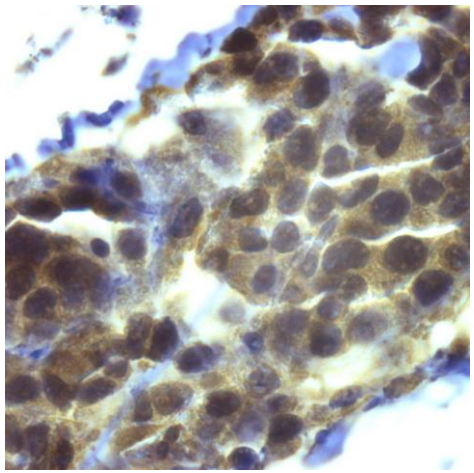

CWR22

B

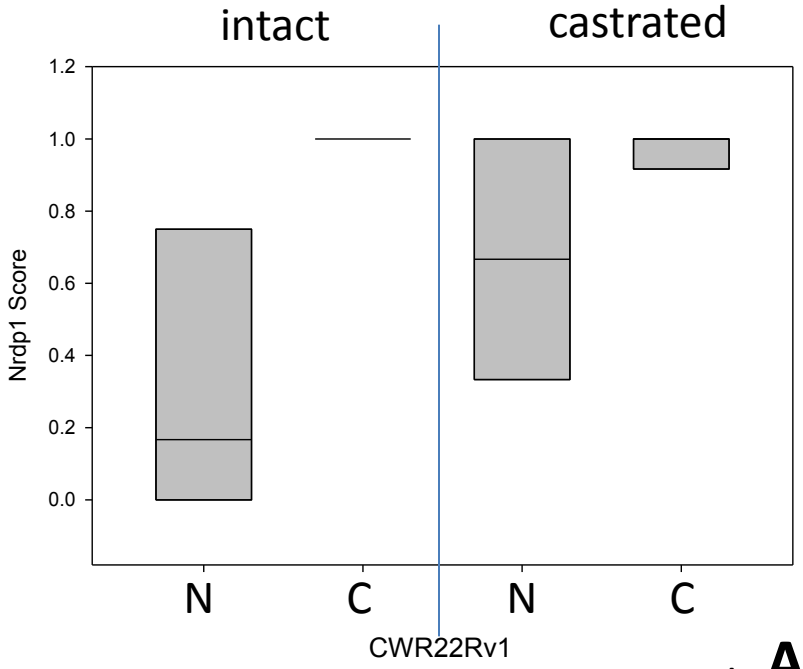

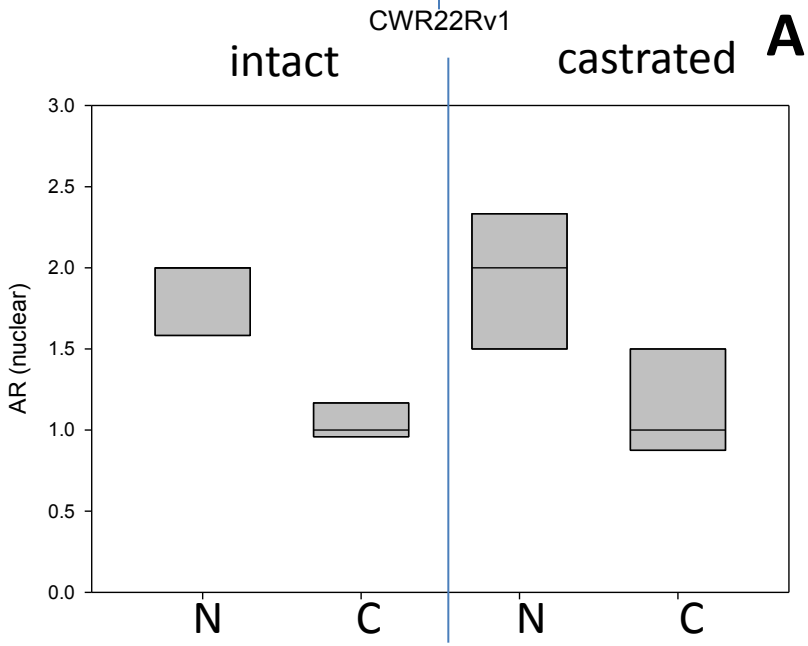

SUPPLEMENTARY FIGURE 5

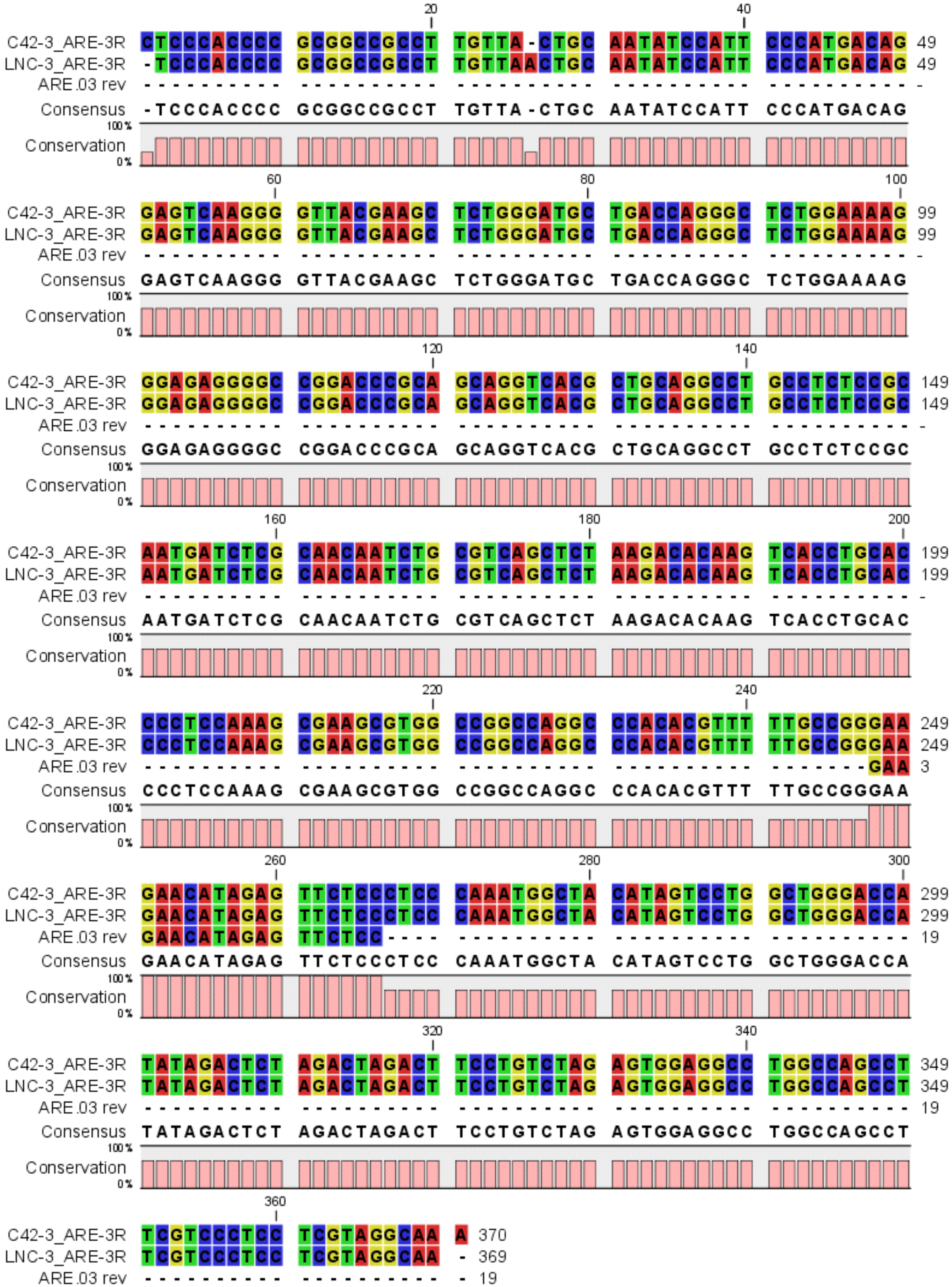

Comparison of ARE.03 sequence of C42 and LNCaP cell lines

SUPPLEMENTARY FIGURE 6

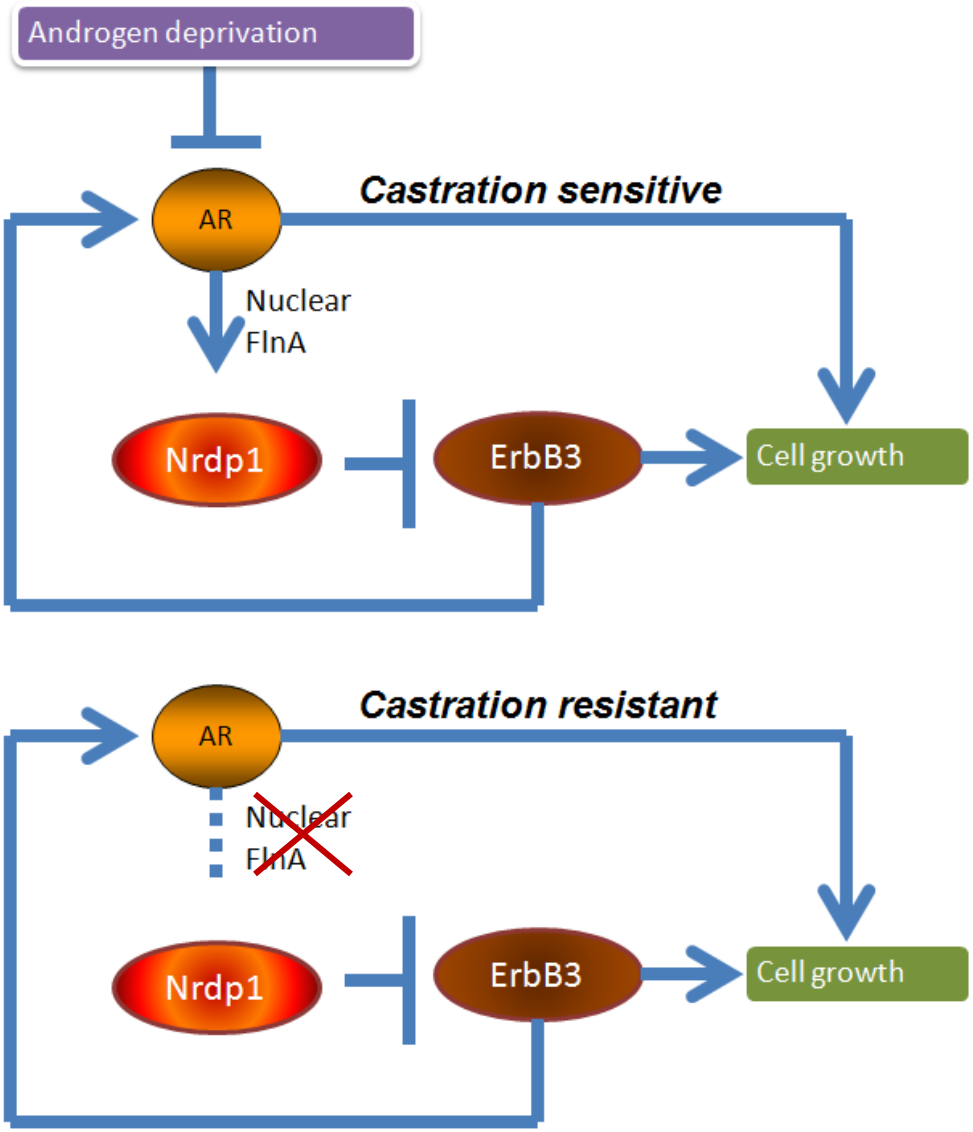

SUPPLEMENTARY FIGURE 7